Article

Cell Systems

Construction and Analysis of Two Genome-Scale Deletion Libraries for *Bacillus subtilis*

Graphical Abstract

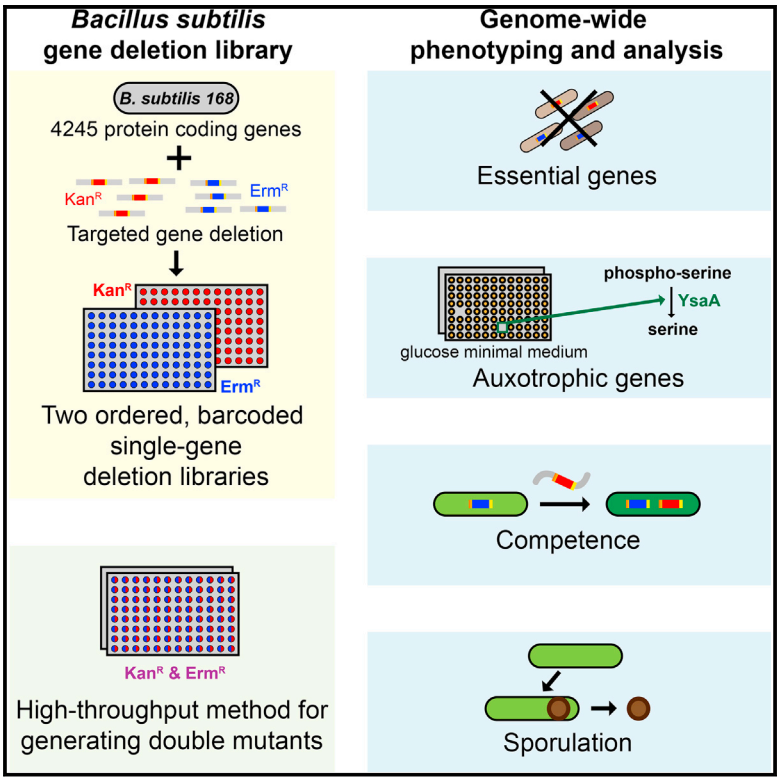

Highlights

- Construction of two ordered gene deletion mutant libraries of *B. subtilis*
- Defined essential and auxotrophic gene sets in *B. subtilis*
- High-throughput methods for transformation and double-mutant analysis
- Genome-wide screening of growth, competence, and sporulation

Authors

Byoung-Mo Koo, George Kritikos, Jeremiah D. Farelli, ..., Karen N. Allen, Athanasios Typas, Carol A. Gross

Correspondence

typas@embl.de (A.T.),
cgrossucsf@gmail.com (C.A.G.)

In Brief

Koo et al. have constructed two complete ordered single-gene deletion mutant libraries of the model Gram-positive model bacterium, *B. subtilis,* and developed new high-throughput methodologies to enable facile screening. They have assessed gene essentiality, auxotrophy, competence, and sporulation genome-wide. These libraries and methods provide versatile resources for the study of gene functions, pathway connections, and their regulation.

Koo et al., 2017, Cell Systems *4*, 1–15
March 22, 2017 © 2017 The Authors. Published by Elsevier Inc.
http://dx.doi.org/10.1016/j.cels.2016.12.013

CellPress

Please cite this article in press as: Koo et al., Construction and Analysis of Two Genome-Scale Deletion Libraries for *Bacillus subtilis*, Cell Systems (2017), http://dx.doi.org/10.1016/j.cels.2016.12.013

Cell Systems
Article

OPEN ACCESS
CellPress

Construction and Analysis of Two Genome-Scale Deletion Libraries for *Bacillus subtilis*

Byoung-Mo Koo,[1] George Kritikos,[4] Jeremiah D. Farelli,[5] Horia Todor,[1] Kenneth Tong,[1] Harvey Kimsey,[6] Ilan Wapinski,[7] Marco Galardini,[8] Angelo Cabal,[1] Jason M. Peters,[1] Anna-Barbara Hachmann,[6] David Z. Rudner,[6] Karen N. Allen,[5] Athanasios Typas,[4,*] and Carol A. Gross[1,2,3,9,*]
[1]Department of Microbiology and Immunology
[2]Department of Cell and Tissue Biology
[3]California Institute of Quantitative Biology
University of California, San Francisco, San Francisco, CA 94158, USA
[4]European Molecular Biology Laboratory, Genome Biology Unit, Meyerhofstrasse 1, 69117 Heidelberg, Germany
[5]Department of Chemistry, Boston University, Boston, MA 02215, USA
[6]Department of Microbiology and Immunobiology, Harvard Medical School, Boston, MA 02115, USA
[7]Department of Systems Biology, Harvard Medical School, Boston, MA 02115, USA
[8]European Bioinformatics Institute, Wellcome Trust Genome Campus, Hinxton, Cambridge CB10 1SD, UK
[9]Lead Contact
*Correspondence: typas@embl.de (A.T.), cgrossucsf@gmail.com (C.A.G.)
http://dx.doi.org/10.1016/j.cels.2016.12.013

SUMMARY

A systems-level understanding of Gram-positive bacteria is important from both an environmental and health perspective and is most easily obtained when high-quality, validated genomic resources are available. To this end, we constructed two ordered, barcoded, erythromycin-resistance- and kanamycin-resistance-marked single-gene deletion libraries of the Gram-positive model organism, *Bacillus subtilis.* The libraries comprise 3,968 and 3,970 genes, respectively, and overlap in all but four genes. Using these libraries, we update the set of essential genes known for this organism, provide a comprehensive compendium of *B. subtilis* auxotrophic genes, and identify genes required for utilizing specific carbon and nitrogen sources, as well as those required for growth at low temperature. We report the identification of enzymes catalyzing several missing steps in amino acid biosynthesis. Finally, we describe a suite of high-throughput phenotyping methodologies and apply them to provide a genome-wide analysis of competence and sporulation. Altogether, we provide versatile resources for studying gene function and pathway and network architecture in Gram-positive bacteria.

INTRODUCTION

The number of sequenced bacterial genes and genomes is increasing exponentially due to new sequencing technologies and microbiome/metagenomic initiatives. Putative gene functions are automatically annotated based on sequence homology to previously characterized genes. However, even in the best-studied bacteria, *Escherichia coli* and *Bacillus subtilis*, >30% of the genes are of unknown function or poorly characterized (Hu et al., 2009; Michna et al., 2014). This deficit limits both the ability to annotate genes by comparative genomics and the ability to harness genomic information to understand and manipulate bacteria.

Phenotypes are key for characterizing gene function and are usually identified by studying the response of a mutant to environmental stress or genetic perturbation. In the genomics era, two approaches are broadly used to map phenotypes in a high-throughput manner: pooled screening of a randomly generated mutant library or characterization of an ordered deletion library (Brochado and Typas, 2013). Transposon mutagenesis followed by pooled screening and analysis using Tn-seq or similar deep-sequencing methodologies is fast and inexpensive and can be utilized in a wide range of bacteria (Gray et al., 2015). However, this technique has several drawbacks: phenotype masking from cross-complementation, biases in strain abundance in the library, inability to deal with bottleneck effects in populations, and the difficulty of phenotype validation and double-mutant analysis. A genome-wide ordered deletion library is labor intensive to construct and must be carefully maintained to avoid cross-contamination but can overcome most limitations of randomly generated libraries, as phenotypes for each mutant can be accurately quantified in isolation. In addition, ordered barcoded libraries can be screened in pooled format, ensuring tighter control of input pool complexity and of bottleneck effects and enabling much higher multiplexing in the sequence readout. Ordered gene deletion mutant libraries are available for several model Gram-negative bacteria (Baba et al., 2006; de Berardinis et al., 2008; Porwollik et al., 2014), and the *E. coli* library has been used for chemical-genomic profiling and double-mutant analysis (Babu et al., 2014; Kumar et al., 2016; Nichols et al., 2011; Shiver et al., 2016).

Gram-positive bacteria are of intense interest because of their diversity of niches, adaptability to environmental extremes, and threat to human health and utility in biotechnology. Nonetheless,

This is an open access article under the CC BY license (http://creativecommons.org/licenses/by/4.0/).

Please cite this article in press as: Koo et al., Construction and Analysis of Two Genome-Scale Deletion Libraries for *Bacillus subtilis*, Cell Systems (2017), http://dx.doi.org/10.1016/j.cels.2016.12.013

Table 1. Summary of Phenotype Screens in This Study

Screen	Outcomes	Points of Screen	Related Figure and/or Dataset
Essential gene	• 257 *B. subtilis* essential genes required for growth in LB at 37°C were defined	detailed procedure for defining essential genes	Table S3, tab A legend
		list of *B. subtilis* essential genes	Table S3, tab A; Figure 2A
	• genome-wide essential gene screen by constructing deletion mutants using two different markers simultaneously	condition essentiality of 30 genes	Table S3, tab A
		discussion of essentiality changes from this study	Table S3, tab B
		comparison of essential genes in *B. subtilis* and other bacteria	Table S3, tab C; Figure 2D
Growth phenotype	• genome-wide relative fitness of libraries in different growth conditions	list of relative fitness (growth phenotypes) of mutants in all conditions	Table S4, tab B
Cold-sensitive (*cs*) phenotype	• genes required for growth in LB at 16°C were identified	list of cold-sensitive mutants and discussion about their phenotypes	Table S4, tab C
	• data suggested that overexpression of some prophage genes are toxic at low temperature	functional groups enriched in *cs* phenotype	Figure S3E
Auxotrophic gene	• genome-wide auxotroph screen identified 98 auxotrophic genes in *B. subtilis*	list of *B. subtilis* auxotrophic genes	Table S4, tab D
		comparison of auxotrophic genes in *B. subtilis* and *E. coli*	Table S4, tab E; Figure 3B
Utilization of carbon (C) or nitrogen (N) source	• genes required for utilizing specific C and N sources were identified	genes required for utilization of specific C or N source	Table S4, tab F
	• several pathway connections in *B. subtilis* metabolism were clarified	analysis of pathways for C or N source utilization in *B. subtilis*	Figure S4
Double-mutant analysis	identification of genes performing the final step of Phe and Tyr biosynthesis	methodology and analysis of linkage effect	Figure 5
		new genes required for Phe and Tyr biosynthesis	Figure S5
Competence	genome-wide competence gene screen identified competence genes in *B. subtilis*	list of competence-defective mutants	Table S5, tab B
		transformability of previously known competence-defective mutants in this study	Table S5, tab C
		conservation of competence genes in other bacteria	Table S5, tab D; Figure S6
Sporulation	genome-wide sporulation screen using colorimetric method confirmed known sporulation mutants and identified new players	list of relative sporulation scores of mutants	Table S6, tab A
		list of sporulation defective mutants	Table S6, tab B
		functional groups enriched in sporulation phenotype	Figure 6E
		conservation of sporulation genes in other bacteria	Table S6, tab E; Figure S7C

with the exception of a single organism with a minimal genome, *Streptococcus sanguinis* (Xu et al., 2011), there has been no systematic effort to elucidate gene function genome-wide in Gram-positive organisms. The Firmicute, *B. subtilis* is the key Gram-positive model organism, with powerful molecular, genetic and cell-biological tools, and several developmental processes: biofilm morphogenesis, competence, and sporulation (Sonenshein et al., 2002). *B. subtilis* and its close relatives are important industrial workhorses, and several *Bacillus* species are pathogenic to humans. Notably, Firmicutes are one of the two most abundant phyla in the human gut microbiome, and the abundance of several of its members has been repeatedly associated with disease (Arumugam et al., 2011; El Feghaly et al., 2015; Miquel et al., 2013).

Here, we report the construction and initial analysis of two *B. subtilis* ordered deletion libraries in which every non-essential gene was replaced with either a kanamycin or an erythromycin resistance cassette (Kan^R or Erm^R libraries). These libraries replace the existing single-gene inactivation library (Kobayashi et al., 2003), which suffered from instability, incomplete coverage, and absence of the standard features of modern libraries. Our libraries are barcoded with easily removable antibiotic markers and suitable for double-mutant analysis. We used these libraries to refine the essential and auxotrophic gene sets, to identify the genes responsible for missing steps in serine, tyrosine, and phenylalanine biosynthesis, and to determine the genes required for low-temperature growth. In addition, we developed and implemented new high-throughput assays, including double-mutant analysis, which allowed us to conduct genome-wide screens for competence and sporulation, two key *B. subtilis* developmental programs (Table 1).

RESULTS AND DISCUSSION

Construction of Single-Gene Deletion Libraries of *B. subtilis* 168

We constructed two comprehensive single-gene deletion libraries of the *B. subtilis* 168 genome (NCBI RefSeq: NC_000964.3) based

Please cite this article in press as: Koo et al., Construction and Analysis of Two Genome-Scale Deletion Libraries for *Bacillus subtilis*, Cell Systems (2017), http://dx.doi.org/10.1016/j.cels.2016.12.013

OPEN ACCESS
CellPress

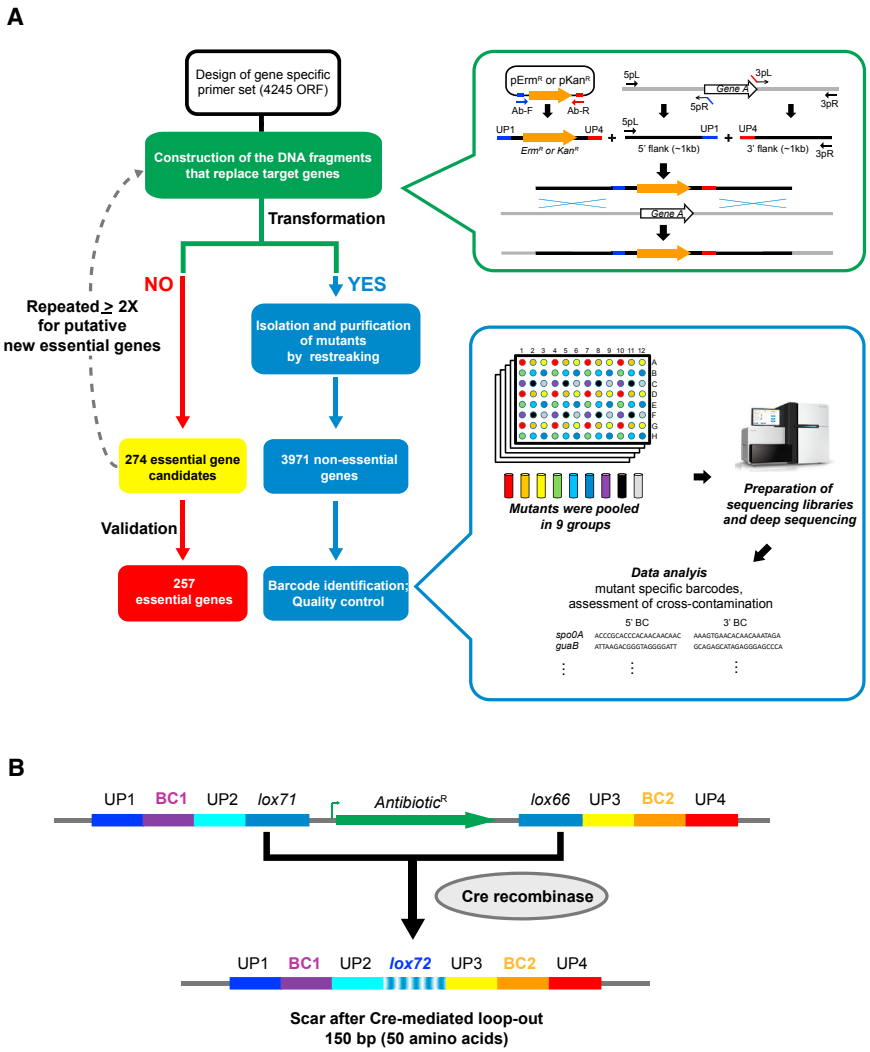

Figure 1. Overview of Construction of Single-Gene Deletion Libraries in *B. subtilis*

(A) Left: Workflow of mutant construction and essential gene validation. Right top (green): Construction of DNA fragments to replace target genes. The plasmid-encoded antibiotic resistance cassette (Erm^R or Kan^R) was amplified with Ab-F and Ab-R, each consisting of a random barcode sequence flanked by UP (Universal priming) sequences. About 1 kb of the 5′ and 3′ flanking sequences of the target gene were amplified by 5pL/5pR and 3pL/3pR, respectively. The purified antibiotic resistance cassette and its flanking regions were joined, amplified, and transformed into the wild-type strain. Right bottom (blue): Schematic procedure for barcode identification. Within each library, mutants were pooled in nine groups as denoted by color code according to their position in 96-well plates. Sequencing libraries were prepared and sequenced as described in STAR Methods. Mutant-specific barcodes were identified by mapping the sequencing reads onto the *B. subtilis* genome. Cross-contamination was indicated when mutant barcodes were present in pools that should lack the mutant. Detailed procedures are described in STAR Methods.

(B) Structure of the antibiotic resistance cassettes. UP1–4, universal priming sequence; BC1 and BC2, mutant-specific barcodes; *lox71* and *lox66*, Cre recombinase recognition sites used for excision of the antibiotic resistance cassette. A150 bp scar sequence after Cre-mediated excision of antibiotic resistance cassette is shown at the bottom. The *lox72* sequence remaining after recombination between *lox71* and *lox66* is indicated.

See also Figure S1 and Tables S1 and S2.

on its natural competence for transformation by linear DNA fragments (Figure 1A). We targeted 4,245 genes for replacement by erythromycin (bacteriostatic) and kanamycin (bactericidal) resistance cassettes. In general, we replaced the entire protein-coding sequence except for the start and stop codons. To minimize functional interference, we maintained at least 21 bp of sequence between the antibiotic resistance cassette and flanking genes, modifying the precise deletion endpoints to maintain this spacing for closely spaced or overlapping genes, or to maintain transcriptional terminators that overlap stop codons (STAR Methods and Table S1).

Using our high-throughput transformation pipeline, we obtained 10–1,000 colonies/transformation, except for when the target was an essential gene. In total, we obtained 3,967 replacements with both antibiotics, as well as four replacements with either Erm^R or Kan^R only, resulting in 3968 Erm^R and 3970 Kan^R mutants. We purified four independent clones of each strain, retained two as frozen stocks, identified barcodes for both isolates (Table S2), and replaced all clones that failed rigorous quality control standards (STAR Methods). We found only two cases of cross-contamination, underlining the high quality of the library and it suitability for further global phenotypic analyses. In contrast to the previously reported *E. coli* and *S. sanguinis* libraries (Baba et al., 2006; Xu et al., 2011), we found no instances of gene duplication, either because we did not enhance recombination during library construction or because of organism-specific differences.

Several features of our antibiotic resistance cassette facilitate downstream analysis (Figure 1B). First, the antibiotic cassettes lack a transcriptional terminator, so that downstream genes in the operon can be transcribed. Second, because transcription from the cassette promoters may modify downstream gene expression and alter phenotypes, the cassette can be excised to alleviate such effects using Cre recombinase sites (Figure S1). Third, Cre cannot utilize the small scar that remains after excision; this facilitates construction of strains with multiple gene deletions (Yan et al., 2008), as demonstrated by making a strain with ten gene deletions from our library (Meeske et al., 2015). Finally, the barcodes and universal priming sites flanking the Cre recognition sites enable ultra-high-throughput deep-sequencing approaches, as recently described for RB-Tn-seq (Wetmore et al., 2015).

To demonstrate the utility of this approach, we determined the phenotypes of the individual mutants comprising both libraries

Please cite this article in press as: Koo et al., Construction and Analysis of Two Genome-Scale Deletion Libraries for *Bacillus subtilis*, Cell Systems (2017), http://dx.doi.org/10.1016/j.cels.2016.12.013

from almost all tested conditions. This allowed us to pinpoint library-specific differences and to report high-confidence phenotypes, i.e., those in common between both libraries. We find high concordance between the two libraries. Discrepancies are rare and probably reflect differential downstream effects of the different antibiotic resistance cassettes or suppressor mutants. Conducting large-scale screens with both libraries largely obviates the problem of false positives. Besides facilitating phenotype validation, two libraries are necessary for high-throughput double-mutant analysis (see below).

The Essential Gene Set

We established the essential gene set in lysogeny broth (LB) at 37°C by starting from the 274 genes that either failed to give transformants after $\geq$2 independent attempts with validated PCR products or produced tiny transformants that did not regrow. Genes that could not be replaced due to secondary effects (e.g., overexpression of an adjacent lethal product by transcription from the promoter of antibiotic resistance gene) and putative new essentials that could not be complemented were excluded from the essential set (see Table S3). We confirmed that new non-essentials lack a copy of the gene that was deleted (STAR Methods).

In total, we defined 257 essential protein-coding genes enriched in several functional categories related to core processes and growth (Figure 2A), including three genes of unknown function: *ylaN* encodes an α-helical bundle protein (Xu et al., 2007); *yneF* encodes a methionine-rich small protein; and *yqeG* encodes a putative HAD family phosphatase (UniProt Consortium, 2015) (Table S3). Compared with the 253 essential genes in the SubtiWiki compendium (http://subtiwiki.uni-goettingen.de/wiki/index.php/Essential_genes), we report 29 new essential and 25 new non-essential genes (Figure 2B and Table S3). Differences likely reflect the fact that ours is the first systematic, high-resolution gene deletion set in *B. subtilis* constructed in a single background strain with consistent techniques by one group. Of the 257 genes essential in LB medium, 30 are not essential in some other growth condition or genomic context (Table S3). LB may have an insufficient amount of particular compounds; e.g., the *ylaN* mutant requires a higher amount of iron than that present in LB (Figure S2) or may lack a compound that could bypass the need for that gene product; e.g., *eno, pgm, gapA*, and *alrA* (Commichau et al., 2013; Heaton et al., 1988). Some gene products are essential only at high growth rates typical of LB at 37°C (*smc* and *scpA*; Gruber et al., 2014), and these may not be essential in the natural soil environment where *B. subtilis* grows slower. Finally, some genes are non-essential in specific genetic backgrounds; e.g., antitoxins can be deleted in strains lacking their cognate toxin gene. Our rationale for the updated list of essential genes is described in detail in Table S3.

Previous comparative studies of essential gene sets (essentialomes) among microbes revealed that the number of essential genes does not scale with genome size; that essential genes are enriched in cell-proliferation-related genes; and that essential genes are preferentially located in operons, usually as the first gene in its operon (Grazziotin et al., 2015). Clade-specific essential genes are usually attributed to distinct surface structures, such as the outer membrane biosynthesis genes in Gram-negative bacteria and teichoic acid biosynthesis genes in Gram-positive bacteria. Having clarified the *B. subtilis* essentialome, we revisited this analysis by comparing the essential genes in four microbes separated by a billion years of evolution (Figure 2C). Three had gold-standard essential gene sets in which targeted gene deletion libraries were used to identify genes required in rich medium (*B. subtilis* [Firmicutes], *S. sanguinis* [Firmicutes] and *E. coli* [γ-proteobacteria]) (Baba et al., 2006; Kato and Hashimoto, 2007; Xu et al., 2011; Yamamoto et al., 2009). The fourth, *S. aureus* (Firmicutes), was defined by transposon mutagenesis. To minimize *S. aureus* false positives, we considered the essential gene set as those essentials present in two independent transposon libraries (Chaudhuri et al., 2009; Santiago et al., 2015).

More than half of the *B. subtilis* essential genes are essential in the other three bacteria, indicating high conservation of essential genes even in distantly related bacteria (Figure 2D, top). Genes involved in translation/ribosome structure and biogenesis are highly enriched ($p = 1.8 \times 10^{-4}$) in this subset (Figure 2D, bottom). An additional 25% of the *B. subtilis* essential genes are present in the other three and variably essential, indicating that they are broadly conserved and important. Interestingly, conservation of essentiality has little to do with phylogeny: the overlap of *B. subtilis* essentials to closely related *S. sanguinis* and distantly related *E. coli* is similar. Broadly distributed genes may not be essential in *B. subtilis* because of the presence of paralogs (e.g., *thrS* and *thrZ* paralogs in *B. subtilis*), differences in the complement of essential nutrient transporters (e.g., *E. coli* lacks a riboflavin transporter), different physiological requirements in different growth conditions (e.g., LB versus tryptic soy agar), or distinct morphological requirements (e.g., *mreC* and *mreD* are essential only in rod-shaped bacteria). The 25% of the *B. subtilis* essential gene set not present in at least one of the other three bacteria is enriched in poorly characterized genes ($p = 6.1 \times 10^{-5}$) and in inorganic ion transport/metabolism ($p = 2.6 \times 10^{-4}$). Their lower conservation results from group-specific essential cell structures and physiology (e.g., envelope and cell division), functionally analogous genes that perform some steps in a pathway, and completely different pathways that carry out the same process (e.g., both the methylerythritol 4- phosphate and mevalonate pathways (Heuston et al., 2012) perform isoprenoid biosynthesis). Detailed results are in Table S3.

In summary, 75% of the *B. subtilis* essential genes are universally present and 50% are universally essential in our four-organism test set, spanning from *E. coli* to *B. subtilis*. In contrast, only 13% of *B. subtilis* genes overall are universally present in the other three organisms. The variably conserved essentials include the 4% of the essential genes that are *B. subtilis* specific, all of which alleviate the lethal activity of other genes (e.g., anti-sigma, anti-toxin, prophage repressor). It is likely that all organisms have a cadre of organism-specific essential genes that improve viability in their natural environment.

Growth Phenotypes in Rich Medium

In this study, we used the integrated colony opacity (Kritikos et al., 2017) to calculate the relative fitness (RF) of each strain in an arrayed screen of the Erm^R and Kan^R libraries (1,536 mutants/plate). LB at 37°C is taken as our standard condition (Table

OPEN ACCESS
CellPress

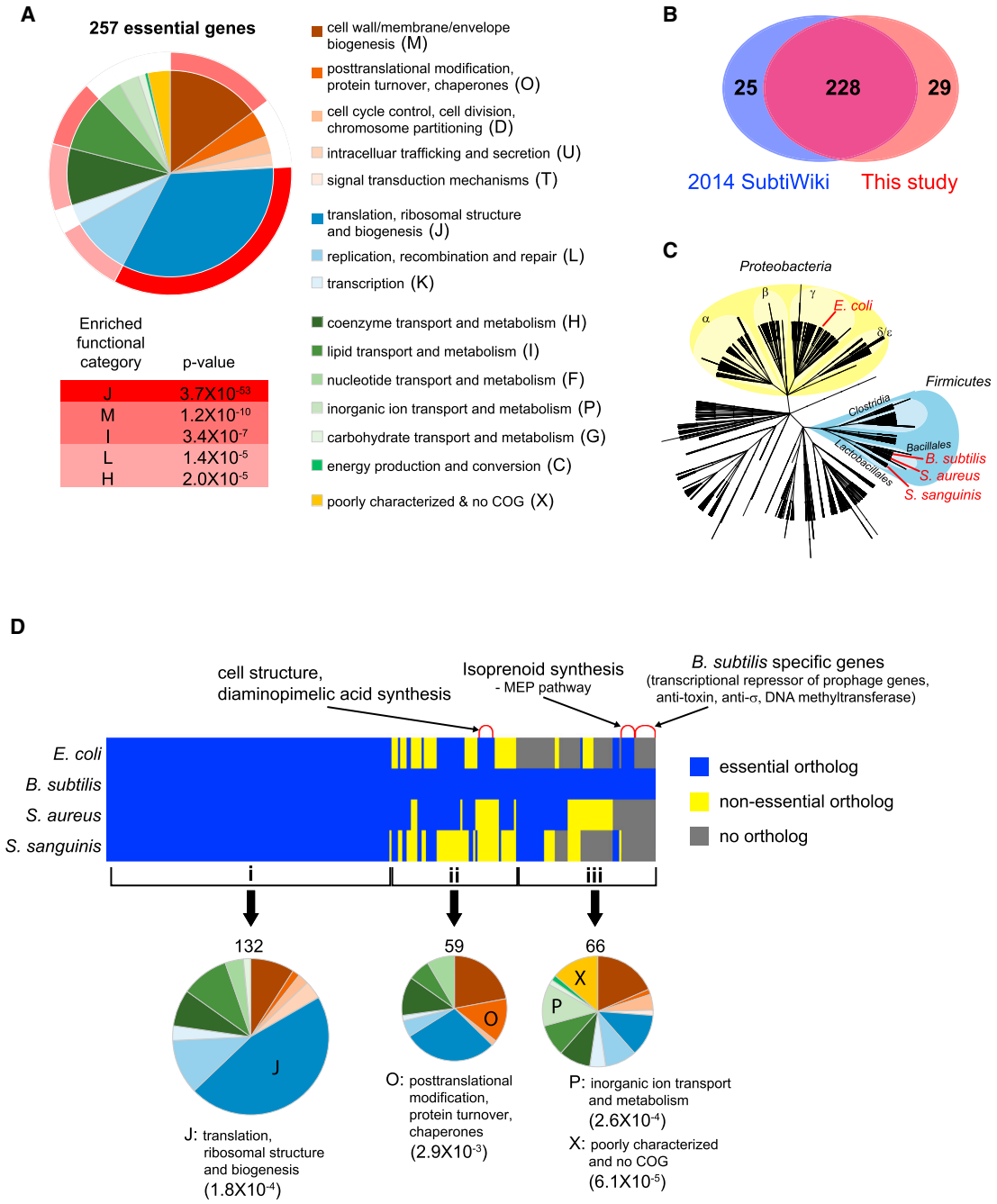

Figure 2. The *B. subtilis* Essential Gene Set

(A) Functional categories of *B. subtilis* essential genes. Pie chart (left) indicates clusters of orthologous groups (COG)-based classification of essential genes. Each color represents a COG class ID described at the right. Gradient red colors outside the pie chart represent enrichment of each category. Bottom table: enriched functional categories of essential genes with their Bonferroni corrected p value.

(B) A Venn diagram comparison of the essential genes from SubtiWiki and our study.

(C) Phylogenetic tree of bacteria representing the distance among *B. subtilis*, *S. aureus*, *S. sanguinis*, and *E. coli*. Two phyla, Firmicutes and Proteobacteria, are highlighted by blue and yellow circles, respectively. The tree was generated from NCBI Taxonomy and visualized in iTOL (Letunic and Bork, 2016).

(D) Conservation and essentiality of orthologs of *B. subtilis* essential genes in *E. coli*, *S. aureus*, and *S. sanguinis*. Top: Orthologs of *B. subtilis* essential genes in other bacteria were identified by pairwise comparison of their protein sequences as determined from their genomic sequences. Genes were grouped by their conservation and essentiality in other bacteria: i, essential in all four bacteria; ii, conserved in all four bacteria; iii, missing in at least one bacterium. Bottom: Pie charts indicate the distribution of functional categories of genes in each group colored according to their COG class IDs shown in (A). The enriched functional categories in each group are indicated by letter in the pie chart; description of enriched functional categories and their Bonferroni corrected p values are indicated under the pie chart.

See also Figure S2 and Table S3.

Please cite this article in press as: Koo et al., Construction and Analysis of Two Genome-Scale Deletion Libraries for *Bacillus subtilis*, Cell Systems (2017), http://dx.doi.org/10.1016/j.cels.2016.12.013

S4), and phenotypes in other conditions are presented as normalized relative fitness (nRF) values: fitness of a strain in condition X relative to that in the standard condition (STAR Methods).

The fitness phenotypes on LB at 37°C were reproducible within and between the Erm^R and Kan^R libraries ($r > 0.67$ and $r = 0.49$; Figures S3A and S3B) with inter-library correlation dropping mostly due to technical reasons and several clone discrepancies. Gene set enrichment analysis (GSEA) (Subramanian et al., 2005) indicates that slower-growing strains are enriched in the energy production/conversion and translation functional categories ($p < 0.05$, Figure S3C). Notably, coenzyme metabolism/transport genes are also enriched among slower-growing strains, suggesting that LB does not have an optimal balance for some cofactors or that cofactors are not taken up well by *B. subtilis*.

We also measured relative fitness at 16°C to identify cold-sensitive mutants (Figure S3D and Table S4). We found enrichment of several gene categories, including translation/ribosome structure and biogenesis and cell cycle control/division/chromosome partitioning (Figure S3E and Table S4).

Growth Phenotypes in Minimal Media

Identification of genes essential for growth in minimal media is important for understanding metabolic pathways and their regulation and provides crucial foundational information for metabolic engineering. *B. subtilis* auxotrophs had previously been inferred from gene annotation. We identified auxotrophic genes by probing the library in glucose-ammonium minimal medium, supplemented with tryptophan to complement the *trpC* mutation in *B. subtilis* 168 (Figure 3A, Table S4). We defined 98 auxotrophs (STAR Methods): 93 experimentally identified auxotrophs, predominantly deleted in known biosynthetic enzymes, but also including *ysaA*, a poorly characterized gene, and the five annotated tryptophan synthesis genes. Auxotrophic genes in *B. subtilis* are as highly biased to the leading strand (91%, $p = 3.9 \times 10^{-5}$) as essential genes (91%, $p = 5.6 \times 10^{-13}$), compared with the leading strand bias of all genes (74%). In contrast, *E. coli* auxotrophic genes lack strand bias, but multi-responsive genes, i.e., genes required in many conditions, are biased toward the leading strand (Nichols et al., 2011). Thus in bacteria, strand bias is thought to be driven by gene essentiality or importance (Nichols et al., 2011; Zheng et al., 2015). The head-on collisions of the replication and transcription machines resulting from lagging strand transcription are deleterious in general and especially deleterious in *B. subtilis* (Merrikh et al., 2012). The strand bias of *B. subtilis* auxotrophic genes would be explained if these genes are essential/important for growth in the natural soil habitat of *B. subtilis*.

Comparison of the 98 *B. subtilis* and the 86 *E. coli* experimentally identified auxotrophic genes (Nichols et al., 2011) indicated an overlap of only 55 genes (Figures 3B and Table S4). This number increased to 59 when the four *B. subtilis* auxotrophs that are essential in *E. coli* (*folD*, *pgk*, *purB*, and *gpsA*) were included, and to 72 when paralogs and redundant pathways were taken into account. The remaining differences reflect genes encoding non-homologous isofunctional enzymes and unique auxotrophic genes, including transcriptional regulators (*gltC* in *B. subtilis* and *lysR* and *metR* in *E. coli*). This diversity may reflect divergent and convergent evolution of enzymes according to their niches (Galperin and Koonin, 2012).

By profiling the mutant library on seven additional C and six N sources, we identified 40 additional genes required for utilization of particular C and N sources and pathway connections in *B. subtilis* central metabolism (Figures 3C and S4, and Table S4).

Identification of the Previously Uncharacterized Gene, YsaA, as a Phosphoserine Phosphatase

In addition to large-scale screens, our libraries may be used to identify the physiological functions of previously uncharacterized genes. As demonstration of this utility, we focused on *ysaA*, which was the only new auxotrophic gene of unknown function. To guide identification of its pathway defect, we grew the *ysaA* mutant in various combinations of amino acids. We found that the *ysaA, serA,* and *serC* mutants have virtually identical profiles when observed across all the conditions we studied, likely placing YsaA in the serine biosynthesis pathway. For example, like other mutants disrupted in serine biosynthesis, the *ysaA* defect was complemented by glycine, or a combination of serine and other amino acids such as glutamine or glutamate. The inability of serine alone to rescue the growth defect of the *serA*, *serC*, or *ysaA* mutants is due to serine toxicity (Lachowicz et al., 1996) (Figure 4A).

In *E. coli*, serine is synthesized either by the GlyA-catalyzed conversion of glycine to serine, or from 3-phosphoglycerate via three enzymatic steps catalyzed by SerA, SerC, and SerB (Figure 4B). Although a *serB* homolog had not been identified in *B. subtilis*, *ysaA* encodes a haloalkanoate dehalogenase superfamily phosphatase. This suggests that *ysaA* may be the *B. subtilis* equivalent of *serB*. Accordingly, we examined the phosphohydrolase activity of YsaA in vitro, screening YsaA against a library of 167 phosphorylated substrates with a stop-point colorimetric assay (Huang et al., 2015). YsaA showed phosphatase activity against phosphoserine, phosphothreonine, phosphoethanolamine, and histidinol phosphate. We measured steady-state kinetic parameters against these substrates and found that YsaA had the highest substrate specificity for phosphoserine with a k_{cat}/K_m of 6.9×10^4 M^{-1} s^{-1} (Figures 4C and 4D), and with a K_m of 0.116 mM, similar to that of *E. coli* SerB (K_m = 0.097 mM) (Kuznetsova et al., 2006).

There is also genetic evidence that *ysaA* and *serB* are functional equivalents. As expected from genes in the same pathway, epistasis experiments show that the *ysaA-serA* and *ysaA-serC* double mutants grew equivalently to each single-mutant strain in glucose-glutamate minimal medium supplemented with serine (Figure 4E). Moreover, although they lack significant amino acid sequence identity, *ysaA* complements *E. coli serB* and vice versa (Figures 4F and 4G), demonstrating that YsaA and SerB are interchangeable in vivo. Given these observations, we rename *ysaA* as *serB*.

High-Throughput Double Gene Mutant Generation

We developed a high-throughput method for generating double mutants in *B. subtilis* based on its natural competence (STAR Methods). The major experimental challenge was the asynchronous development of competence due to the widely different growth rates of the library in competence medium. We solved this problem by adding DNA at the time of inoculation and growing overnight prior to enriching for transformants

OPEN ACCESS
CellPress

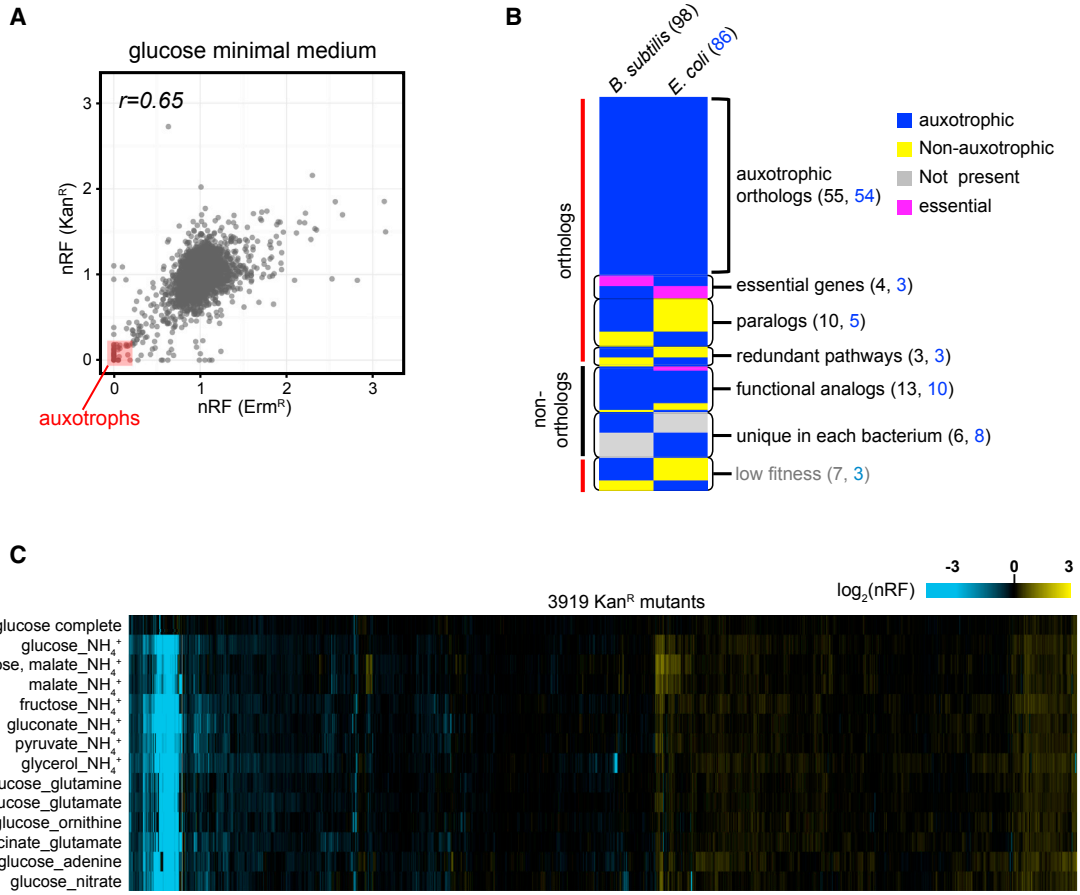

Figure 3. Profiling of Strain Fitness in Minimal Media

The Erm^R and Kan^R libraries arrayed in high density (1,536/plate) were grown in minimal media with different C or N source. We used integrated colony opacity (Iris; Kritikos et al., 2017) to calculate the normalized relative fitness (nRF) of each mutant (colony opacity of mutant)/(median colony opacity in plate). Data were processed as described in STAR Methods and are listed in Table S4.

(A) Scatterplot of the nRF of Erm^R and Kan^R mutants in glucose minimal medium at 37°C. We defined as auxotrophs mutants with an nRF <0.3 in both libraries (red square).

(B) Comparison of auxotrophic genes in *B. subtilis* and *E. coli*. Orthologs were identified by pairwise protein sequence alignments using NCBI BLAST. The Metacyc database (Caspi et al., 2014) was used for functional annotation of genes and pathway analysis. The colors represent conservation, essentiality, and auxotrophy of genes in each bacterium. The reasons for discordance in auxotrophy between orthologs are described to the right of the chart. The numbers of auxotrophic genes in each category for *B. subtilis* (black) and *E. coli* (blue) are indicated.

(C) Heatmap representation of nRF of 3911 Kan^R mutants (x axis) in 13 minimal media conditions and in defined rich medium (y axis).

See also Figures S3 and S4 and Table S4.

(Figure 5A). *hisC::kan* genomic DNA successfully transformed 3,811 of 3,899 Erm^R gene deletion strains (69 strains were missing from this screen), indicating that our method is suitable for high-throughput generation of double mutants. As *hisC* contributes to the last step of phenylalanine (Phe) and tyrosine (Tyr) biosynthesis, as well as histidine (His) biosynthesis, we were able to use the results of this screen to identify double mutants that required Phe/Tyr as well as His to grow. Coupled with downstream analysis, we found that *yhdR*, renamed *pheC*, is a major aminotransferase catalyzing this reaction and that AspB also plays a minor catalytic role in producing Phe and Tyr (Figure S5 and Table S5).

Double-mutant analysis is generally limited by linkage, which precludes constructing double mutants that are nearby on DNA because one of the two mutants will be recombined out. We determined the genetic distance necessary to obtain double mutants at reasonable frequency by systematically introducing a second mutation to a strain in which an adjacent or near adjacent gene was marked with a different antibiotic marker. Using two different genomic contexts (*amyE* and *gmuD*), we found that the gene immediately adjacent to the locus being transformed lost its existing antibiotic marker, but those only two or three genes away maintained their markers to a large degree (>20%) (Figure 5B). The efficiency reached ~40% at a distance of three genes (~2 kb), at which point there is a negligible effect on the resultant double-mutant strains. Thus, linkage effects are minimal compared with other microbes (50–200 kb in *E. coli*, fission or budding yeast) (Collins et al., 2006; Roguev et al., 2007; Typas

OPEN ACCESS
CellPress

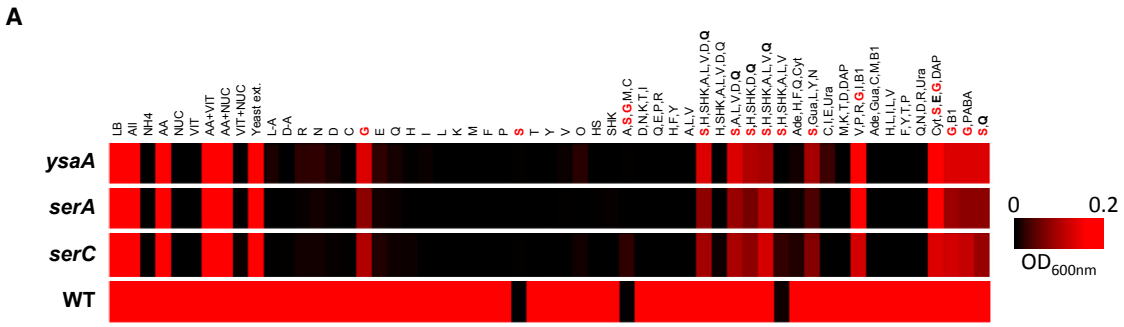

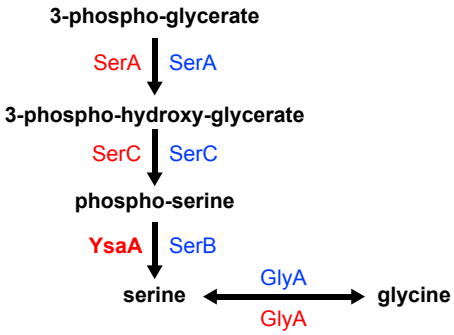

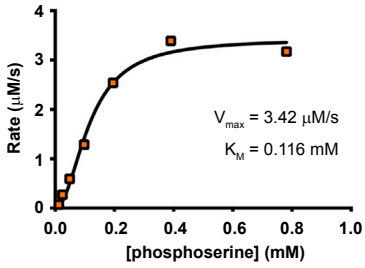

D

substrate	k_{cat} (s^{-1})	K_M (mM)	k_{cat}/K_M ($M^{-1}s^{-1}$)
phosphoserine	6.9 ± 0.1	0.116 ± 0.01	5.9×10^4
phosphothreonine	9.5 ± 0.1	2.91 ± 0.15	3.2×10^3
phosphoethanolamine	7.9 ± 0.1	4.20 ± 0.16	1.8×10^3
histidinol phosphate	7.1 ± 0.1	2.65 ± 0.40	1.3×10^3

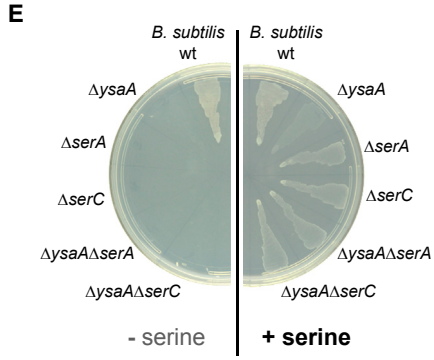

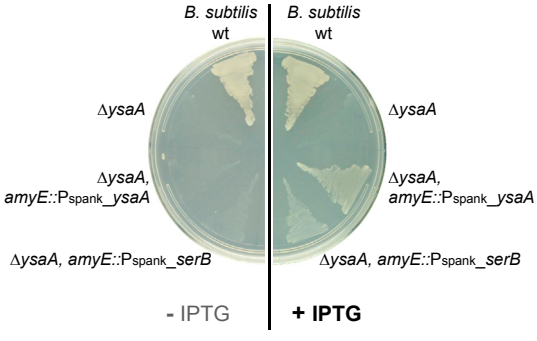

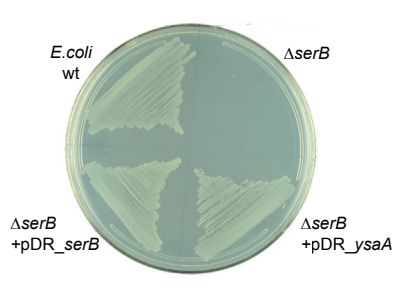

Figure 4. Identifying the Function of YsaA

(A) Growth of *ysaA*, *serA*, *serC*, and wild-type in various defined media are shown as a heatmap. Values are based on the average of duplicate determinations of the OD_{600} of each strain after 18 hr in glucose minimal media supplemented with various metabolites and pools of metabolites. Amino acids are represented by their single letter code. Abbreviations: AA, amino acids; NUC, nucleoside bases; VIT, vitamins; L-A, L-alanine; D-A, D-alanine; HS, homoserine; SHK, shikimate; Ade, adenine; Cyt, cytosine; Gua, guanine; Ura, uracil; DAP, diaminopimelic acid; B1, vitamin B1; PABA, p-amino benzoic acid.

(legend continued on next page)

OPEN ACCESS
CellPress

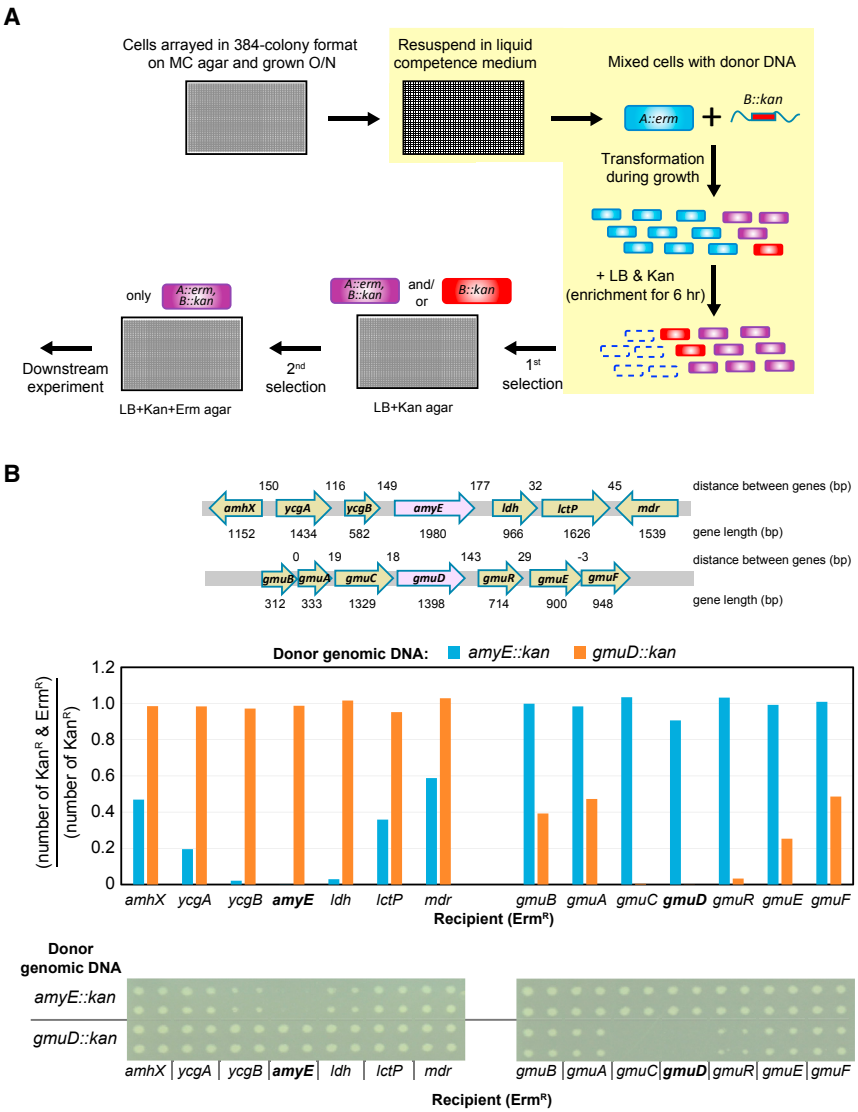

Figure 5. High-Throughput Transformation with Genomic DNA

(A) Schematic procedure for high-throughput double-mutant generation. Erm^R mutants arrayed in 384 format on MC agar plates were re-suspended in liquid competence medium, mixed with genomic DNA from donor (*Kan*^{R}), and incubated for 16 hr. Transformants were then enriched by adding LB and kanamycin and incubation for 6 hr further. Note that mutants with only Kan^R can also be generated by replacement of the Erm^R region with its original wild-type sequence, which results from co-transformation of the wild-type piece of genomic DNA (congression). Following enrichment for transformants on Kan, double mutants (Kan^R + Erm^R) were selected on both erythromycin and kanamycin. The steps in liquid medium are highlighted in yellow. The genome-wide screen was performed with *hisC:kan*.

(B) The minimum distance between deletions in a double mutant was assessed by determining the fraction of mutants in the *amyE* or *gmuD* neighborhood that maintained their Erm^R antibiotic marker after transformation with *amyE*::*Kan*^{R} and *gmuD*::*Kan*^{R} genomic DNA. This experiment was performed according to the protocol in (A) except that the enrichment step was eliminated to obtain an accurate estimation of the number of transformants that retained both markers. Top: Genomic context of the *amyE* and *gmu*D loci. Middle: Quantitative representation of the results. A bar graph indicating the fraction of double mutants among total transformants. Results at the *amyE* locus (left) and the *gmuD* locus (right). Bottom: Qualitative representation of the results. Direct plating of the double mutants in each transformation presented in the bar graph. Each plating is in duplicate from technical replicate cultures.

See also Figures S5 and S6 and Table S5.

et al., 2008), enabling such high-resolution coverage of genetic interactions for the first time. We anticipate that this methodology and our libraries will be used extensively in the future for high-throughput genetic interaction profiling in *B. subtilis*.

Competence

Competence is an important developmental state in *B. subtilis*, but no genome-wide screens have been performed to identify all the players necessary for DNA uptake and other steps in the process. Using our new high-throughput method for generating double mutants, our transformation of the Erm^R gene deletion library with *hisC::kan* genomic DNA identified 88 mutants that failed to be transformed (Table S5). These 88 mutants included most identified competence genes. Because this qualitative assay contains an enrichment step, it cannot score gradations of competence. Fifteen known competence-defective mutants, mostly involved in signaling pathways to regulate ComK (Hamoen et al., 2003) were deemed competent proficient in this

(B) Serine biosynthesis pathway. Known enzymes catalyzing each step in *B. subtilis* (red) and *E. coli* (blue) are shown. The function of YsaA (bold) was identified as part of this study.

(C) Saturation curve for phosphoserine phosphatase activity of YsaA.

(D) Steady-state kinetic parameters for YsaA against four putative substrates.

(E) Epistatic interaction of *ysaA* with *serA* and *serC* in *B. subtilis* is shown by comparing plates with (right) or without (left) serine.

(F) Complementation of *B. subtilis ysaA* with either *B. subtilis ysaA* or with *E.coli serB*, each integrated at the *B. subtilis amyE* chromosomal locus, and controlled by an isopropyl β-D-1-thiogalactopyranoside (IPTG)-inducible promoter (P_{spank}).

(G) Complementation of *E. coli serB* growing in glucose minimal medium with multicopy plasmids expressing *B. subtilis ysaA* (pDR_*yasA*) or *E.coli serB* (pDR_*serB*).

OPEN ACCESS
CellPress

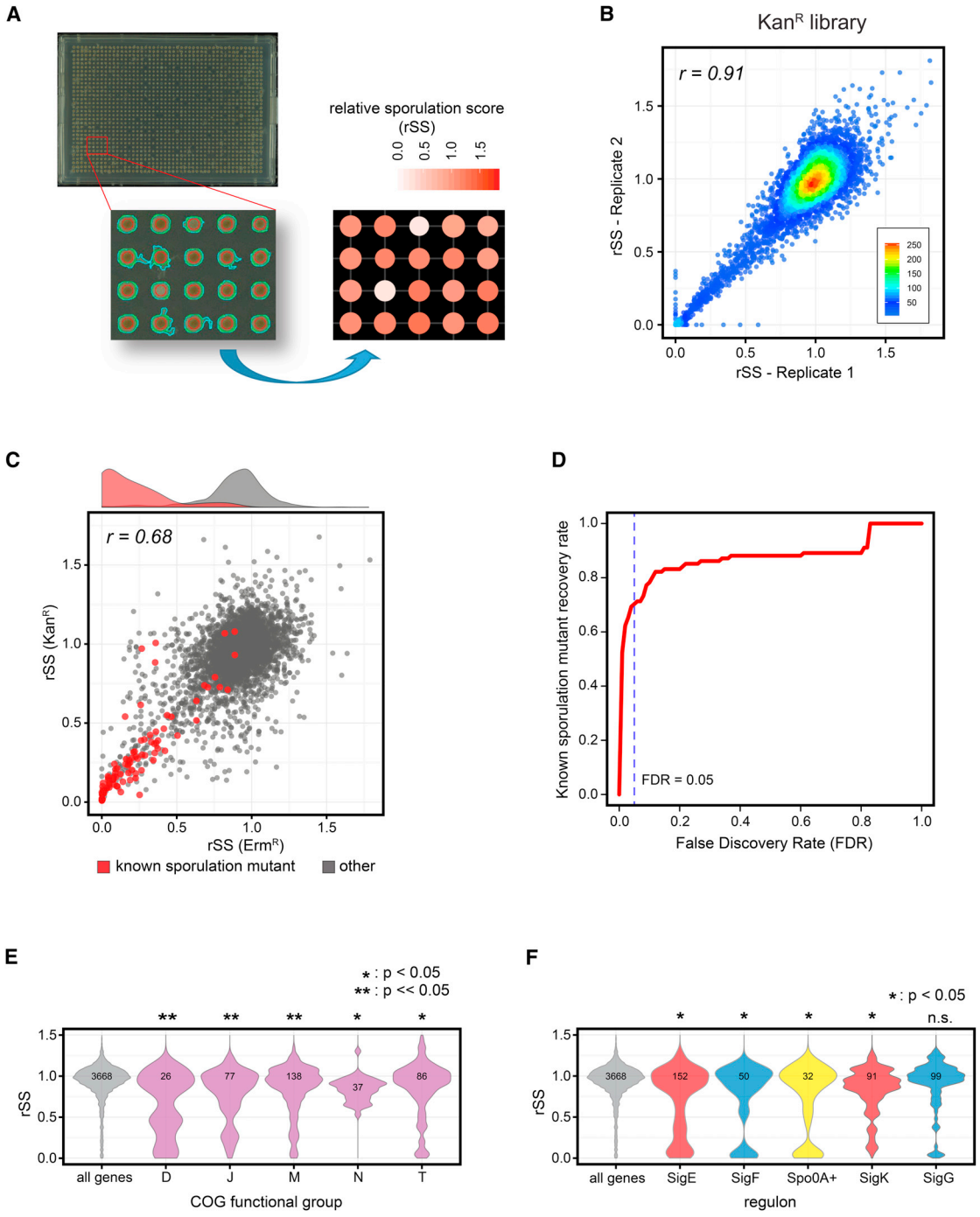

Figure 6. Genome-wide Screening of Sporulation in *B. subtilis*

(A) Sporulation phenotypes and colony size were automatically quantified using Iris (Kritikos et al., 2017) after 45 hr of growth on succinate-glutamate minimal agar plates supplemented with limiting amounts of nutrients. Top: A representative sporulation plate image is shown. Bottom left: A zoomed-in portion of the 1,536 colony array image processed with Iris is shown at the lower left. The raw sporulation score is calculated from the color intensity in the center area of the colony (red circle). Bottom right: Color-coded relative sporulation scores (rSS) of each mutant in the zoomed-in portion are shown. rSS was calculated by the following equation: rSS = (sporulation score of mutant)/(median sporulation score in plate). For details see STAR Methods.

(B) Reproducibility of rSS from two technical replicates of the Kan^R library.

(C) The rSS of Erm^R and Kan^R mutants is shown by scatter plot, with the sporulation scores of 101 known sporulation mutants indicated in red color. A density plot (above) indicates the relative distribution of known mutants compared with all genes in *B. subtilis*.

(D) Using a 5% FDR, 70% of the known sporulation mutants were recovered in this screen.

(legend continued on next page)

assay, likely because they reduced rather than abolished competence (Table S5).

To provide further semi-quantitative competence information, we compared competence with and without enrichment (STAR Methods). Testing the competence mutant candidates identified from the genome-wide screen described above and strains missing from that screen yielded 61 non-transformable or poorly transformable strains, of which 34 were previously known to be competence defective (Table S5). These 34 genes are involved in DNA uptake and recombination, membrane proteolysis, mRNA degradation, and control of the amount, activity, and stability of ComK, the master competence regulator. The remaining 27 competence-defective strains comprised nine strains that are strong candidates for new competence genes and 18 strains that are growth impaired and did not reach the cell density required for competence development in our medium. Of these nine new putative competence genes, four are also involved in other processes (*greA*, *prmC*, *pgi*, and *ptsI*) but are likely to also have a competence-specific role and are present in all naturally transformable strains we queried (Figure S6 and Table S5). The other five are poorly characterized and confined to Bacillales. Since the regulation of competence development diversifies rapidly even within the same genus, we suggest that the function of these genes is related to *B. subtilis*-specific competence development.

Sporulation

Sporulation is the major developmental pathway in *Bacilli* and *Clostridia*, and an important survival strategy for both pathogenic and microbiome members of these genera (Browne et al., 2016; Jedrzejas, 2002). This pathway has been heavily studied, starting with the isolation of individual mutants that do not sporulate. In *B. subtilis*, such studies had identified the key sporulation-related transcription factors, regulons, and inter-compartmental communication strategies (Higgins and Dworkin, 2012). Nearly 25% of the genome has been associated with this process (~1,000 genes; Eijlander et al., 2014).

However, lack of a comprehensive mutant library and a high-throughput assay had prevented genome-wide sporulation phenotyping. We developed a high-throughput assay to assess sporulation based on the dark brown color produced by sporulating cells in minimal medium at a late stage of sporulation (Driks, 1999) (Figure 6A and STAR Methods), and then applied it to our mutant library to determine the relative contributions of known and new sporulation genes in our two libraries (Table S6).

Our sporulation assay was reproducible ($r > 0.9$ for technical replicates and $r = 0.68$ for biological replicates from the two libraries) and captured the majority of the known sporulation mutants (Figures 6B, 6C, and S7A). Poorly growing and non-reproducible mutants were filtered from the dataset and removed from subsequent analysis (STAR Methods, Figure S7B, and Table S6). Of the 101 known sporulation mutants present in the filtered data, we recovered 71 at 5% false discovery rate (FDR) and 79 at 10% FDR (Figure 6D). We did not expect to recover 10 of the remaining 22 sporulation mutants either because they had medium-specific defects or because they were involved in producing dipicolinic acid for spore heat resistance, a step that is independent of pigment development. We recovered genes encoding the quorum-sensing peptides *phrA* and *phrE*, transcriptional regulators and sporulation sigmas, the sporulation phosphorelay, the *spo0A* phosphorylation-stimulating complex, and most *spo* genes (Table S6). Notably, the *phrA* and *phrE* mutants would be lost in a pooled screen as they would be complemented by the predominantly wild-type cells in the population (Meeske et al., 2016).

Using a stringent 5% FDR cutoff ($rSS < 0.31$), we also identified an additional 73 genes likely to be sporulation defective of which 33 are poorly characterized, and 40 are of known function. We and others validated 12 of these players (Table S6) (Meeske et al., 2016), with two of the poorly characterized genes, *ywmB* (*spoIIT*) and *yqzE* (*spoIIIL*), being identified as forespore activators of SigE and SigG (Meeske et al., 2016). Further examination of the newly identified sporulation genes revealed new connections and roles. Two of the poorly characterized cell-envelope-related genes, *yabM* and *ykvU*, encode paralogs of the MurJ and SpoVB lipid II flippases (Meeske et al., 2015). Based on our results and their previous associations with cell-wall-related phenotypes (Vasudevan et al., 2009), we speculate that both play a specialized, flippase-related role in spore cortex synthesis. Among the known signal transduction genes, *yqfL* is a negative regulator of the CcpN gluconeogenesis repressor (Servant et al., 2005). As CcpN negatively regulates *gapB* (Servant et al., 2005), a gluconeogenic enzyme whose deletion also results in a sporulation defect, we suggest that gluconeogenesis may have a direct impact on sporulation. Finally, 15/40 known genes are involved in translation. That a significant fraction (6/15) of the non-essential ribosomal protein genes analyzed in this screen have sporulation phenotypes suggests either that they have a specific role in sporulation or that they are needed in stressful circumstances. In support of the former idea, these deletion strains were not cold sensitive (Table S4), a condition where translation is compromised (Barria et al., 2013).

To obtain an overall overview of the processes involved in sporulation, we identified functional categories enriched in low sporulation scores. GSEA analysis identified cell cycle/division, cell envelope biogenesis, signal transduction, translation, and cell motility as enriched functional categories ($p < 0.05$, Figure 6E). It will be interesting to determine in the future whether the role of these processes in sporulation requires additional protein synthesis, and also whether they are necessary in both the mother cell and forespore. We also assessed the importance of genes in the known *spo* regulons to sporulation using GSEA analysis

(E) COG functional groups enriched in sporulation-defective mutants ($p < 0.05$). A violin plot showing the distribution of the rSS of genes by functional group with the total member of genes in each category indicated. Width represents the probability density of the data at a given rSS. D, cell cycle control, cell division, chromosome partitioning; J, translation, ribosome structure, and biogenesis; M, cell wall/membrane/envelope biogenesis; N, cell motility; T, signal transduction. (F) Distribution of the rSS of genes positively regulated by mother-cell sporulation sigmas (SigE and SigK; red), forespore sigmas (SigF and SigG; blue), and Spo0A (yellow). Total number of genes in each category is indicated. Sigma regulons enriched in sporulation-defective genes are indicated by *; $p < 0.05$); n.s., not significant.
See also Figure S7 and Table S6.

Please cite this article in press as: Koo et al., Construction and Analysis of Two Genome-Scale Deletion Libraries for *Bacillus subtilis*, Cell Systems (2017), http://dx.doi.org/10.1016/j.cels.2016.12.013

of the regulons of Spo0A, which initiates sporulation, and the sporulation sigma factors, SigE, F, K, and G (Eijlander et al., 2014). As expected, all of these regulons are enriched in our hits ($p < 0.05$), with the exception of SigG (Figure 6F), which has a role in the terminal processes of sporulation. Only 52/407 genes, or 10%–20% of the genes in each regulon, are significantly sporulation defective (rSS < 0.31), consistent with the previous findings on the SigE regulon (Eichenberger et al., 2003). Notably, genes expressed in the mother cell (SigE or SigK regulons) are just as likely as those expressed in the forespore (SigF or SigG regulons) to have severe phenotypes (Figure 6F), indicating the important role of the mother cell in nourishing and orchestrating forespore development, and the equal redundancy of function on both compartments. Mutants in *spo* regulons with no or weak phenotypes may have subtle, conditional, or redundant effects. These genes require additional dissection, possibly by double-mutant analysis (Silvaggi et al., 2004), which can now be performed with the high-throughput method described above.

We used our genome-scale dataset of 144 known and newly identified sporulation genes to reexamine the genetic signature for sporulating Firmicutes (Figure S7C and Table S6). Previous genomic studies comparing sporulating and non-sporulating Firmicutes (*Bacilli* + *Clostridia*) identified 50–60 genes that comprised a genetic signature for sporulating Firmicute, as well as a larger set of *Bacilli*- or *Clostridia*-specific sporulation genes (Abecasis et al., 2013; Galperin et al., 2012). We confirmed the previously identified genetic signature for sporulating Firmicutes and identified two new broadly conserved sporulation genes, *disA* and *minD*. *disA* was previously implicated in reporting about DNA integrity during sporulation, but no *spo* phenotype had been identified (Bejerano-Sagie et al., 2006). *minD* was just identified as a member of complex machinery for proper chromosome segregation with a mild *spo* phenotype (Kloosterman et al., 2016).

We confirmed the known *Bacilli*-specific sporulation genes and identified several new members of this group. In addition to *ywmB*, *yqzE*, and *ykvU*, discussed above, we identify *yppC*, *ywgA*, *yunG*, *rsiX*, and *kinB* as *Bacilli*-specific sporulation genes. *kinB* is involved in sporulation signal transduction but was not thought to have a sporulation phenotype (Trach and Hoch, 1993). Our study also identified two secreted signaling short peptides (PhrI and PhrK), known to play roles in other processes (Auchtung et al., 2006, 2007), as potentially defective in sporulation as well. Although direct conservation analysis is difficult because the peptides are short, each Phr inhibits an adjacent response regulator aspartate phosphatase (Rap). We find that *rap-phr* gene pairs are widely present in sporulating *Bacillus* species but absent in sporulating *Clostridia* and even in closely related non-sporulating *Listeria monocytogenes*, suggesting that they play a species-specific role in regulation of sporulation.

Perspectives

We report the construction of two ordered *B. subtilis* single-gene deletion libraries, accompanied by high-throughput technologies that will facilitate functional genomics in the premier model Gram-positive bacterium. This platform will also nucleate studies in related Firmicutes of importance for human health and industrial technologies.

We refined the essential gene subset, provided the first comprehensive characterization of auxotrophic genes, and assessed competence and sporulation genome wide. Our studies were performed with both the Kan^R and Erm^R libraries, finding high phenotypic agreement. The few discrepancies arose from different strengths of the promoters driving Erm and Kan expression, occasionally resulting in different downstream effects, and suppressive mutations masking the phenotype of especially sick mutants (e.g., *ponA*, *pdhA*, and *fmt*; Table S4). The simplest way to ensure a valid phenotype is to screen both libraries for the phenotypes of interest. The Bacillus Genetic Stock Center (BGSC, www.bgsc.org) is already distributing individual Erm^R mutants and will soon be able to distribute the Kan^R mutants. The entire Kan^R library will also be distributed by Addgene.

Our libraries have several important features. The antibiotic resistance cassette can easily be removed via the Cre/lox system, and removal can be performed sequentially thereby enabling dissection of gene redundancy. The library is optimal for arrayed screens, which are necessary for assaying single-cell phenotypes that cannot be identified in pooled screens, including screens for genes involved in morphology, sporulation, and production of secreted proteins, secondary metabolites, and antibiotics. In addition, as each mutant has two unique barcodes that are retained even after removal of the antibiotic resistance cassette, this collection is a critical resource for high-throughput pooled studies. Like RB-Tn-seq (Wetmore et al., 2015), library preparation is simple, increasing throughput. In addition, our barcoded library is significantly less complex (only one barcode/gene) versus >100,000 mutants in a typical Tn-seq screen, further increasing throughput so that it is feasible to test relative fitness in hundreds of conditions in one sequencing lane. These libraries also permit adjusting complexity of the initial pools to bypass potential bottleneck effects (Maier et al., 2014). Finally, each mutation can be easily transferred to different *B. subtilis* genetic backgrounds to study traits lost from the domesticated strain, such as surface swarming and the formation of architecturally complex biofilms (Zeigler et al., 2008).

The rapid identification of gene functions, pathways, and their regulation in divergent bacteria is a major challenge in microbiology and has spawned a cadre of high-throughput phenotyping approaches, including comparative genomics, proteomics, high-throughput enzyme activity screens, metabolomics, and functional genomics. We demonstrated the synergy of these approaches in our identification of the function of the auxotrophic gene, *ysaA*, renamed *serB*. The next goal is to integrate data from diverse approaches to build a high-resolution biological network. Using the same resource library will facilitate data integration. Indeed, several groups are using our library for transcriptomics, ribosome profiling, cell imaging, and chemical genetics.

STAR★METHODS

Detailed methods are provided in the online version of this paper and include the following:

- KEY RESOURCES TABLE
- CONTACT FOR REAGENT AND RESOURCE SHARING
- EXPERIMENTAL MODEL AND SUBJECT DETAILS
- METHOD DETAILS
  - Design of Primers
  - Construction of Single Gene Deletion Mutants

SUPPLEMENTAL INFORMATION

Supplemental Information includes seven figures and six tables can be found with this article online at http://dx.doi.org/10.1016/j.cels.2016.12.013.

AUTHOR CONTRIBUTIONS

Conceptualization, B.M.K., D.Z.R., A.T., and C.A.G.; Methodology, B.M.K., G.K., J.D.F., D.Z.R., K.N.A., A.T., and C.A.G.; Investigation, B.M.K., G.K., J.D.F., K.T., J.M.P., H.K., A.C., A.-B.H., and D.Z.R.; Formal Analysis, B.M.K., G.K., J.D.F., H.T., I.W., M.G., D.Z.R., K.N.A., A.T., and C.A.G.; Writing – Original Draft, B.M.K., G.K., H.T., K.N.A., A.T., and C.A.G.; Writing – Review & Editing, B.M.K., G.K., H.T., A.T., and C.A.G.; Funding Acquisition, D.Z.R., K.N.A., A.T., and C.A.G.; Supervision, B.M.K., D.Z.R., K.N.A., A.T., and C.A.G.

ACKNOWLEDGMENTS

We thank D. Dubnau, K.C. Huang, B.M. Burton, A.D. Grossman, A.L. Sonenshein, and members of the Gross laboratory for helpful comments. This work was supported by Sofja Kovalevskaja award to A.T.; NIH U54 GM093342 to K.N.A.; NIH RC2 GM092616 to C.A.G. and D.Z.R.; NIH R01 GM073831 to D.Z.R.; NIH R01 GM102790 and R35 GM118061 to C.A.G.

Received: July 2, 2016
Revised: November 19, 2016
Accepted: December 21, 2016
Published: February 8, 2017

SUPPORTING CITATIONS

The following references appear in the Supplemental Information: Barak et al., 1996; Kanehisa et al., 2014; Nester and Montoya, 1976; Yoshida et al., 2003.

REFERENCES

Abecasis, A.B., Serrano, M., Alves, R., Quintais, L., Pereira-Leal, J.B., and Henriques, A.O. (2013). A genomic signature and the identification of new sporulation genes. J. Bacteriol. *195*, 2101–2115.

Altschul, S.F., Gish, W., Miller, W., Myers, E.W., and Lipman, D.J. (1990). Basic local alignment search tool. J. Mol. Biol. *215*, 403–410.

Arumugam, M., Raes, J., Pelletier, E., Le Paslier, D., Yamada, T., Mende, D.R., Fernandes, G.R., Tap, J., Bruls, T., Batto, J.M., et al. (2011). Enterotypes of the human gut microbiome. Nature *473*, 174–180.

Auchtung, J.M., Lee, C.A., and Grossman, A.D. (2006). Modulation of the ComA-dependent quorum response in *Bacillus subtilis* by multiple Rap proteins and Phr peptides. J. Bacteriol. *188*, 5273–5285.

Auchtung, J.M., Lee, C.A., Garrison, K.L., and Grossman, A.D. (2007). Identification and characterization of the immunity repressor (ImmR) that controls the mobile genetic element ICEBs1 of *Bacillus subtilis*. Mol. Microbiol. *64*, 1515–1528.

Baba, T., Ara, T., Hasegawa, M., Takai, Y., Okumura, Y., Baba, M., Datsenko, K.A., Tomita, M., Wanner, B.L., and Mori, H. (2006). Construction of *Escherichia coli* K-12 in-frame, single-gene knockout mutants: the Keio collection. Mol. Syst. Biol. *2*, 2006 0008.

Babu, M., Arnold, R., Bundalovic-Torma, C., Gagarinova, A., Wong, K.S., Kumar, A., Stewart, G., Samanfar, B., Aoki, H., Wagih, O., et al. (2014). Quantitative genome-wide genetic interaction screens reveal global epistatic relationships of protein complexes in *Escherichia coli*. PLoS Genet. *10*, e1004120.

Barak, I., Behari, J., Olmedo, G., Guzman, P., Brown, D.P., Castro, E., Walker, D., Westpheling, J., and Youngman, P. (1996). Structure and function of the Bacillus SpoIIE protein and its localization to sites of sporulation septum assembly. Mol. Microbiol. *19*, 1047–1060.

Barria, C., Malecki, M., and Arraiano, C.M. (2013). Bacterial adaptation to cold. Microbiology *159*, 2437–2443.

Bejerano-Sagie, M., Oppenheimer-Shaanan, Y., Berlatzky, I., Rouvinski, A., Meyerovich, M., and Ben-Yehuda, S. (2006). A checkpoint protein that scans the chromosome for damage at the start of sporulation in *Bacillus subtilis*. Cell *125*, 679–690.

Brochado, A.R., and Typas, A. (2013). High-throughput approaches to understanding gene function and mapping network architecture in bacteria. Curr. Opin. Microbiol. *16*, 199–206.

Browne, H.P., Forster, S.C., Anonye, B.O., Kumar, N., Neville, B.A., Stares, M.D., Goulding, D., and Lawley, T.D. (2016). Culturing of 'unculturable' human microbiota reveals novel taxa and extensive sporulation. Nature *533*, 543–546.

Caspi, R., Altman, T., Billington, R., Dreher, K., Foerster, H., Fulcher, C.A., Holland, T.A., Keseler, I.M., Kothari, A., Kubo, A., et al. (2014). The MetaCyc database of metabolic pathways and enzymes and the BioCyc collection of Pathway/Genome Databases. Nucleic Acids Res. *42*, D459–D471.

Chaudhuri, R.R., Allen, A.G., Owen, P.J., Shalom, G., Stone, K., Harrison, M., Burgis, T.A., Lockyer, M., Garcia-Lara, J., Foster, S.J., et al. (2009). Comprehensive identification of essential *Staphylococcus aureus* genes using Transposon-Mediated Differential Hybridisation (TMDH). BMC Genomics *10*, 291.

Collins, S.R., Schuldiner, M., Krogan, N.J., and Weissman, J.S. (2006). A strategy for extracting and analyzing large-scale quantitative epistatic interaction data. Genome Biol. *7*, R63.

Commichau, F.M., Pietack, N., and Stulke, J. (2013). Essential genes in *Bacillus subtilis*: a re-evaluation after ten years. Mol. Biosyst. *9*, 1068–1075.

de Berardinis, V., Vallenet, D., Castelli, V., Besnard, M., Pinet, A., Cruaud, C., Samair, S., Lechaplais, C., Gyapay, G., Richez, C., et al. (2008). A complete collection of single-gene deletion mutants of *Acinetobacter baylyi* ADP1. Mol. Syst. Biol. *4*, 174.

Driks, A. (1999). *Bacillus subtilis* spore coat. Microbiol. Mol. Biol. Rev. *63*, 1–20.

Eichenberger, P., Jensen, S.T., Conlon, E.M., van Ooij, C., Silvaggi, J., Gonzalez-Pastor, J.E., Fujita, M., Ben-Yehuda, S., Stragier, P., Liu, J.S., et al. (2003). The sigmaE regulon and the identification of additional sporulation genes in *Bacillus subtilis*. J. Mol. Biol. *327*, 945–972.

Eijlander, R.T., de Jong, A., Krawczyk, A.O., Holsappel, S., and Kuipers, O.P. (2014). SporeWeb: an interactive journey through the complete sporulation cycle of *Bacillus subtilis*. Nucleic Acids Res. *42*, D685–D691.

El Feghaly, R.E., Bangar, H., and Haslam, D.B. (2015). The molecular basis of *Clostridium difficile* disease and host response. Curr. Opin. Gastroenterol. *31*, 24–29.

Galperin, M.Y., and Koonin, E.V. (2012). Divergence and convergence in enzyme evolution. J. Biol. Chem. *287*, 21–28.

Galperin, M.Y., Mekhedov, S.L., Puigbo, P., Smirnov, S., Wolf, Y.I., and Rigden, D.J. (2012). Genomic determinants of sporulation in *Bacilli* and *Clostridia*: towards the minimal set of sporulation-specific genes. Environ. Microbiol. *14*, 2870–2890.

Please cite this article in press as: Koo et al., Construction and Analysis of Two Genome-Scale Deletion Libraries for *Bacillus subtilis*, Cell Systems (2017), http://dx.doi.org/10.1016/j.cels.2016.12.013

Gray, A.N., Koo, B.M., Shiver, A.L., Peters, J.M., Osadnik, H., and Gross, C.A. (2015). High-throughput bacterial functional genomics in the sequencing era. Curr. Opin. Microbiol. *27*, 86–95.

Grazziotin, A.L., Vidal, N.M., and Venancio, T.M. (2015). Uncovering major genomic features of essential genes in Bacteria and a methanogenic Archaea. FEBS J. *282*, 3395–3411.

Gruber, S., Veening, J.W., Bach, J., Blettinger, M., Bramkamp, M., and Errington, J. (2014). Interlinked sister chromosomes arise in the absence of condensin during fast replication in *B. subtilis*. Curr. Biol. *24*, 293–298.

Hamoen, L.W., Venema, G., and Kuipers, O.P. (2003). Controlling competence in *Bacillus subtilis*: shared use of regulators. Microbiology *149*, 9–17.

Heaton, M.P., Johnston, R.B., and Thompson, T.L. (1988). Controlled lysis of bacterial cells utilizing mutants with defective synthesis of D-alanine. Can. J. Microbiol. *34*, 256–261.

Heuston, S., Begley, M., Gahan, C.G., and Hill, C. (2012). Isoprenoid biosynthesis in bacterial pathogens. Microbiology *158*, 1389–1401.

Higgins, D., and Dworkin, J. (2012). Recent progress in *Bacillus subtilis* sporulation. FEMS Microbiol. Rev. *36*, 131–148.

Hu, P., Janga, S.C., Babu, M., Diaz-Mejia, J.J., Butland, G., Yang, W., Pogoutse, O., Guo, X., Phanse, S., Wong, P., et al. (2009). Global functional atlas of *Escherichia coli* encompassing previously uncharacterized proteins. PLoS Biol. *7*, e96.

Huang, H., Pandya, C., Liu, C., Al-Obaidi, N.F., Wang, M., Zheng, L., Toews Keating, S., Aono, M., Love, J.D., Evans, B., et al. (2015). Panoramic view of a superfamily of phosphatases through substrate profiling. Proc. Natl. Acad. Sci. USA *112*, E1974–E1983.

Huerta-Cepas, J., Szklarczyk, D., Forslund, K., Cook, H., Heller, D., Walter, M.C., Rattei, T., Mende, D.R., Sunagawa, S., Kuhn, M., et al. (2016). eggNOG 4.5: a hierarchical orthology framework with improved functional annotations for eukaryotic, prokaryotic and viral sequences. Nucleic Acids Res. *44*, D286–D293.

Jedrzejas, M.J. (2002). The structure and function of novel proteins of *Bacillus anthracis* and other spore-forming bacteria: development of novel prophylactic and therapeutic agents. Crit. Rev. Biochem. Mol. Biol. *37*, 339–373.

Kanehisa, M., Goto, S., Sato, Y., Kawashima, M., Furumichi, M., and Tanabe, M. (2014). Data, information, knowledge and principle: back to metabolism in KEGG. Nucleic Acids Res. *42*, D199–D205.

Kato, J., and Hashimoto, M. (2007). Construction of consecutive deletions of the *Escherichia coli* chromosome. Mol. Syst. Biol. *3*, 132.

Kloosterman, T.G., Lenarcic, R., Willis, C.R., Roberts, D.M., Hamoen, L.W., Errington, J., and Wu, L.J. (2016). Complex polar machinery required for proper chromosome segregation in vegetative and sporulating cells of *Bacillus subtilis*. Mol. Microbiol. *101*, 333–350.

Kobayashi, K., Ehrlich, S.D., Albertini, A., Amati, G., Andersen, K.K., Arnaud, M., Asai, K., Ashikaga, S., Aymerich, S., Bessieres, P., et al. (2003). Essential *Bacillus subtilis* genes. Proc. Natl. Acad. Sci. USA *100*, 4678–4683.

Kritikos, G., Banzhaf, M., Herrera-Dominguez, L., Koumoutsi, A., Wartel, M., Zietek, M., and Typas, A. (2017). A tool named Iris for versatile high-throughput phenotyping in microorganisms. Nat. Microbiol. nmicrobiol.2017.14.

Kumar, A., Beloglazova, N., Bundalovic-Torma, C., Phanse, S., Deineko, V., Gagarinova, A., Musso, G., Vlasblom, J., Lemak, S., Hooshyar, M., et al. (2016). Conditional epistatic interaction maps reveal global functional rewiring of genome integrity pathways in *Escherichia coli*. Cell Rep. *14*, 648–661.

Kuznetsova, E., Proudfoot, M., Gonzalez, C.F., Brown, G., Omelchenko, M.V., Borozan, I., Carmel, L., Wolf, Y.I., Mori, H., Savchenko, A.V., et al. (2006). Genome-wide analysis of substrate specificities of the *Escherichia coli* haloacid dehalogenase-like phosphatase family. J. Biol. Chem. *281*, 36149–36161.

Lachowicz, T.M., Morzejko, E., Panek, E., and Piatkowski, J. (1996). Inhibitory action of serine on growth of bacteria of the genus *Bacillus* on mineral synthetic media. Folia Microbiol. *41*, 21–25.

Langmead, B., and Salzberg, S.L. (2012). Fast gapped-read alignment with Bowtie 2. Nat. Methods *9*, 357–359.

Letunic, I., and Bork, P. (2016). Interactive tree of life (iTOL) v3: an online tool for the display and annotation of phylogenetic and other trees. Nucleic Acids Res. *44*, W242–W245.

Maier, L., Diard, M., Sellin, M.E., Chouffane, E.S., Trautwein-Weidner, K., Periaswamy, B., Slack, E., Dolowschiak, T., Stecher, B., Loverdo, C., et al. (2014). Granulocytes impose a tight bottleneck upon the gut luminal pathogen population during *Salmonella typhimurium* colitis. PLoS Pathog. *10*, e1004557.

Meeske, A.J., Sham, L.T., Kimsey, H., Koo, B.M., Gross, C.A., Bernhardt, T.G., and Rudner, D.Z. (2015). MurJ and a novel lipid II flippase are required for cell wall biogenesis in *Bacillus subtilis*. Proc. Natl. Acad. Sci. USA *112*, 6437–6442.

Meeske, A.J., Rodrigues, C.D., Brady, J., Lim, H.C., Bernhardt, T.G., and Rudner, D.Z. (2016). High-throughput genetic screens identify a large and diverse collection of new sporulation genes in *Bacillus subtilis*. PLoS Biol. *14*, e1002341.

Mende, D.R., Sunagawa, S., Zeller, G., and Bork, P. (2013). Accurate and universal delineation of prokaryotic species. Nat. Methods *10*, 881–884.

Merrikh, H., Zhang, Y., Grossman, A.D., and Wang, J.D. (2012). Replication-transcription conflicts in bacteria. Nat. Rev. Microbiol. *10*, 449–458.

Michna, R.H., Commichau, F.M., Todter, D., Zschiedrich, C.P., and Stulke, J. (2014). SubtiWiki-a database for the model organism *Bacillus subtilis* that links pathway, interaction and expression information. Nucleic Acids Res. *42*, D692–D698.

Miquel, S., Martin, R., Rossi, O., Bermudez-Humaran, L.G., Chatel, J.M., Sokol, H., Thomas, M., Wells, J.M., and Langella, P. (2013). *Faecalibacterium prausnitzii* and human intestinal health. Curr. Opin. Microbiol. *16*, 255–261.

Nester, E.W., and Montoya, A.L. (1976). An enzyme common to histidine and aromatic amino acid biosynthesis in *Bacillus subtilis*. J. Bacteriol. *126*, 699–705.

Nichols, R.J., Sen, S., Choo, Y.J., Beltrao, P., Zietek, M., Chaba, R., Lee, S., Kazmierczak, K.M., Lee, K.J., Wong, A., et al. (2011). Phenotypic landscape of a bacterial cell. Cell *144*, 143–156.

O'Leary, N.A., Wright, M.W., Brister, J.R., Ciufo, S., Haddad, D., McVeigh, R., Rajput, B., Robbertse, B., Smith-White, B., Ako-Adjei, D., et al. (2016). Reference sequence (RefSeq) database at NCBI: current status, taxonomic expansion, and functional annotation. Nucleic Acids Res. *44*, D733–D745.

Porwollik, S., Santiviago, C.A., Cheng, P., Long, F., Desai, P., Fredlund, J., Srikumar, S., Silva, C.A., Chu, W., Chen, X., et al. (2014). Defined single-gene and multi-gene deletion mutant collections in *Salmonella enterica* sv Typhimurium. PLoS One *9*, e99820.

Roguev, A., Wiren, M., Weissman, J.S., and Krogan, N.J. (2007). High-throughput genetic interaction mapping in the fission yeast *Schizosaccharomyces pombe*. Nat. Methods *4*, 861–866.

Santiago, M., Matano, L.M., Moussa, S.H., Gilmore, M.S., Walker, S., and Meredith, T.C. (2015). A new platform for ultra-high density *Staphylococcus aureus* transposon libraries. BMC Genomics *16*, 252.

Servant, P., Le Coq, D., and Aymerich, S. (2005). CcpN (YqzB), a novel regulator for CcpA-independent catabolite repression of *Bacillus subtilis* gluconeogenic genes. Mol. Microbiol. *55*, 1435–1451.

Shiver, A.L., Osadnik, H., Kritikos, G., Li, B., Krogan, N., Typas, A., and Gross, C.A. (2016). A chemical-genomic screen of neglected antibiotics reveals illicit transport of kasugamycin and Blasticidin S. PLoS Genet. *12*, e1006124.

Silvaggi, J.M., Popham, D.L., Driks, A., Eichenberger, P., and Losick, R. (2004). Unmasking novel sporulation genes in *Bacillus subtilis*. J. Bacteriol. *186*, 8089–8095.

Son, M.S., and Taylor, R.K. (2011). Preparing DNA libraries for multiplexed paired-end deep sequencing for Illumina GA sequencers. Curr. Protoc. Microbiol. *Chapter 1*. Unit 1E.4.

Sonenshein, A.L., Hoch, J.A., and Losick, R. (2002). *Bacillus subtilis* and Its Closest Relatives: From Genes to Cells (ASM Press).

Subramanian, A., Tamayo, P., Mootha, V.K., Mukherjee, S., Ebert, B.L., Gillette, M.A., Paulovich, A., Pomeroy, S.L., Golub, T.R., Lander, E.S., et al. (2005). Gene set enrichment analysis: a knowledge-based approach for

interpreting genome-wide expression profiles. Proc. Natl. Acad. Sci. USA *102*, 15545–15550.

Trach, K.A., and Hoch, J.A. (1993). Multisensory activation of the phosphorelay initiating sporulation in *Bacillus subtilis*: identification and sequence of the protein kinase of the alternate pathway. Mol. Microbiol. *8*, 69–79.

Typas, A., Nichols, R.J., Siegele, D.A., Shales, M., Collins, S.R., Lim, B., Braberg, H., Yamamoto, N., Takeuchi, R., Wanner, B.L., et al. (2008). High-throughput, quantitative analyses of genetic interactions in *E. coli*. Nat. Methods *5*, 781–787.

UniProt Consortium. (2015). UniProt: a hub for protein information. Nucleic Acids Res. *43*, D204–D212.

Untergasser, A., Cutcutache, I., Koressaar, T., Ye, J., Faircloth, B.C., Remm, M., and Rozen, S.G. (2012). Primer3–new capabilities and interfaces. Nucleic Acids Res. *40*, e115.

Vallenet, D., Belda, E., Calteau, A., Cruveiller, S., Engelen, S., Lajus, A., Le Fevre, F., Longin, C., Mornico, D., Roche, D., et al. (2013). MicroScope–an integrated microbial resource for the curation and comparative analysis of genomic and metabolic data. Nucleic Acids Res. *41*, D636–D647.

Vasudevan, P., McElligott, J., Attkisson, C., Betteken, M., and Popham, D.L. (2009). Homologues of the *Bacillus subtilis* SpoVB protein are involved in cell wall metabolism. J. Bacteriol. *191*, 6012–6019.

Wetmore, K.M., Price, M.N., Waters, R.J., Lamson, J.S., He, J., Hoover, C.A., Blow, M.J., Bristow, J., Butland, G., Arkin, A.P., et al. (2015). Rapid quantification of mutant fitness in diverse bacteria by sequencing randomly bar-coded transposons. MBio *6*, e00306–e00315.

Xu, L., Sedelnikova, S.E., Baker, P.J., Hunt, A., Errington, J., and Rice, D.W. (2007). Crystal structure of *S. aureus* YlaN, an essential leucine rich protein involved in the control of cell shape. Proteins *68*, 438–445.

Xu, P., Ge, X., Chen, L., Wang, X., Dou, Y., Xu, J.Z., Patel, J.R., Stone, V., Trinh, M., Evans, K., et al. (2011). Genome-wide essential gene identification in *Streptococcus sanguinis*. Sci. Rep. *1*, 125.

Yamamoto, N., Nakahigashi, K., Nakamichi, T., Yoshino, M., Takai, Y., Touda, Y., Furubayashi, A., Kinjyo, S., Dose, H., Hasegawa, M., et al. (2009). Update on the Keio collection of *Escherichia coli* single-gene deletion mutants. Mol. Syst. Biol. *5*, 335.

Yan, X., Yu, H.J., Hong, Q., and Li, S.P. (2008). Cre/lox system and PCR-based genome engineering in *Bacillus subtilis*. Appl. Environ. Microbiol. *74*, 5556–5562.

Yoshida, K., Yamaguchi, H., Kinehara, M., Ohki, Y.H., Nakaura, Y., and Fujita, Y. (2003). Identification of additional TnrA-regulated genes of *Bacillus subtilis* associated with a TnrA box. Mol. Microbiol. *49*, 157–165.

Zeigler, D.R., Pragai, Z., Rodriguez, S., Chevreux, B., Muffler, A., Albert, T., Bai, R., Wyss, M., and Perkins, J.B. (2008). The origins of 168, W23, and other *Bacillus subtilis* legacy strains. J. Bacteriol. *190*, 6983–6995.

Zheng, W.X., Luo, C.S., Deng, Y.Y., and Guo, F.B. (2015). Essentiality drives the orientation bias of bacterial genes in a continuous manner. Sci. Rep. *5*, 16431.

Zlitni, S., Ferruccio, L.F., and Brown, E.D. (2013). Metabolic suppression identifies new antibacterial inhibitors under nutrient limitation. Nat. Chem. Biol. *9*, 796–804.

Please cite this article in press as: Koo et al., Construction and Analysis of Two Genome-Scale Deletion Libraries for *Bacillus subtilis*, Cell Systems (2017), http://dx.doi.org/10.1016/j.cels.2016.12.013

STAR★METHODS

KEY RESOURCES TABLE

Reagent or Resource	Source	Identifier
Chemicals, Peptides, and Recombinant Proteins		
Lysogeny broth (LB), Lennox	Fisher scientific	Cat# BP1427-2
Tryptic Soy Agar (TSA)	BD Biosciences	Cat# 236950
Nutrient broth	BD Biosciences	Cat# 234000
Agar	BD Biosciences	Cat# 214030
Hemin	Sigma-Aldrich	Cat# 51280
Yeast extract	BD Biosciences	Cat# 212750
Casamino acids	BD Biosciences	Cat# 223050
Potassium phosphate monobasic	Sigma-Aldrich	Cat# P0662
Potassium phosphate dibasic	Sigma-Aldrich	Cat# P8281
Trisodium citrate dihydrate	Fisher scientific	Cat# S279-500
Ferric ammonium citrate	Sigma-Aldrich	Cat# F5879
Potassium glutamate monohydrate	Sigma-Aldrich	Cat# G1501
Potassium aspartate	Sigma-Aldrich	Cat# A6558
Manganese chloride tetrahydrate	Sigma-Aldrich	Cat# M3634
Magnesium sulfate heptahydrate	Sigma-Aldrich	Cat# M1880
L-tryptophan	Fisher scientific	Cat# BP395-100
Dextrose (D-[+]-glucose)	Sigma-Aldrich	Cat# D9434
IPTG	Denville scientific	Cat# C18280-13
MOPS	Sigma-Aldrich	Cat# M1254
Potassium sulfate	Sigma-Aldrich	Cat# P9458
Ammonium Chloride	Sigma-Aldrich	Cat# A9434
L-alanine	Sigma-Aldrich	Cat# A7627
D-alanine	Sigma-Aldrich	Cat# A7377
L-arginine	Sigma-Aldrich	Cat# A8094
L-glutamine	Sigma-Aldrich	Cat# G3126
Glycine	Sigma-Aldrich	Cat# G7126
L-histidine	Sigma-Aldrich	Cat# H8125
L-isoleucine	Sigma-Aldrich	Cat# I2752
L-leucine	Sigma-Aldrich	Cat# L8000
L-lysine	Sigma-Aldrich	Cat# L5626
L-methionine	Sigma-Aldrich	Cat# M9625
L-proline	Sigma-Aldrich	Cat# P0380
L-serine	Sigma-Aldrich	Cat# S4500
L-threonine	Sigma-Aldrich	Cat# T8625
L-valine	Sigma-Aldrich	Cat# V0500
L-cysteine hydrochloride monohydrate	Sigma-Aldrich	Cat# C7880
L-phenylalanine	Sigma-Aldrich	Cat# P2126
L-tyrosine	Sigma-Aldrich	Cat# T3754
p-amino benzoic acid	Sigma-Aldrich	Cat# A9878
p-hydroxy benzoic acid	Sigma-Aldrich	Cat# H5376
2,6-diaminopimelic acid	Sigma-Aldrich	Cat# D1377
L-Homoserine	Sigma-Aldrich	Cat# H6515
Shikimic acid	Sigma-Aldrich	Cat# S5375
Adenine	Sigma-Aldrich	Cat# A8626

(*Continued on next page*)

Continued

Reagent or Resource	Source	Identifier
Cytosine	Sigma-Aldrich	Cat# C3506
Guanine	Sigma-Aldrich	Cat# G11950
Uracil	Sigma-Aldrich	Cat# U0750
Biotin	Sigma-Aldrich	Cat# B4501
Nicotinamide	Sigma-Aldrich	Cat# N3376
(-)-Riboflavin	Sigma-Aldrich	Cat# R9504
Thiamine hydrochloride	Sigma-Aldrich	Cat# T4625
Calcium pantothenate	Sigma-Aldrich	Cat# C8731
Pyridoxine hydrochloride	Sigma-Aldrich	Cat# P6280
Vitamine B_{12}	Sigma-Aldrich	Cat# V2876
Succinic acid	Sigma-Aldrich	Cat# S3674
D-(-)-Fructose	Sigma-Aldrich	Cat# F0127
L-(-)-malic acid sodium salt	Sigma-Aldrich	Cat# M1125
Glycerol	Fisher scientific	Cat# G30-4
Sodium pyruvate	Sigma-Aldrich	Cat# P2256
D-gluconic acid	Sigma-Aldrich	Cat# G9005
L-ornithine	Sigma-Aldrich	Cat# O2375
Potassium nitrate	Sigma-Aldrich	Cat# P8394
Calcium chloride dihydrate	Sigma-Aldrich	Cat# C3881
Zinc chloride	Sigma-Aldrich	Cat# 208086
Cobalt(II) chloride hexahydrate	Sigma-Aldrich	Cat# 60820
Sodium molybdate dihydrate	Sigma-Aldrich	Cat# 71756
Copper(II) chloride dihydrate	Sigma-Aldrich	Cat# 307483
Ferric chloride hexahydrate	Sigma-Aldrich	Cat# F2877
2,2'-dipyridyl	Sigma-Aldrich	Cat# D216305
Kanamycin sulfate	Sigma-Aldrich	Cat# K1377
Erythromycin	Sigma-Aldrich	Cat# E5389
Lincomycin hydrochloride	Sigma-Aldrich	Cat# L2774
Spectinomycin dihydrochloride pentahydrate	Sigma-Aldrich	Cat# S9007
Ampicillin sodium salt	Sigma-Aldrich	Cat# A9518
SalI-HF (restriction enzyme)	New England Biolabs	Cat# R3138
HindIII-HF (restriction enzyme)	New England Biolabs	Cat# R3104
NheI-HF (restriction enzyme)	New England Biolabs	Cat# R3131
SphI-HF (restriction enzyme)	New England Biolabs	Cat# R3182
Phusion hot-start DNA polymerase	Thermo scientific	Cat# F540L
Q5 High-Fidelity DNA polymerase	New England Biolabs	Cat# M0491L
T4 DNA ligase	New England Biolabs	M0202
T4 DNA polymerase	New England Biolabs	M0203
DNA polymerase I, Large (Klenow) Fragment	New England Biolabs	M0210
T4 Polynucleotide kinase	New England Biolabs	M0201
Klenow fragment (3' → 5' exo-)	New England Biolabs	M0212
dATP solution	New England Biolabs	N0440
dNTP solution mix	New England Biolabs	N0447
Lysozyme (from chicken egg white)	Sigma-Aldrich	Cat# L6876
Triton X-100	Fisher scientific	Cat# BP151-500
Imidazole	Sigma-Aldrich	Cat# I2399
DTT (DL-dithiothreitol)	Sigma-Aldrich	Cat# D9779

(*Continued on next page*)

Please cite this article in press as: Koo et al., Construction and Analysis of Two Genome-Scale Deletion Libraries for *Bacillus subtilis*, Cell Systems (2017), http://dx.doi.org/10.1016/j.cels.2016.12.013

Continued

Reagent or Resource	Source	Identifier
HEPES	Sigma-Aldrich	Cat# H3375
Tris(2-carboxyethyl)phosphine hydrochloride, (TCEP)	Sigma-Aldrich	Cat# C4706
2-mercaptoethanol	Sigma-Aldrich	Cat# M3148
Biomol Green	Enzo Life Sciences	Cat# BML AK111
Critical Commercial Assays		
Agencourt AMPure XP	Beckman Coulter	Cat# A63881
Dynabeads MyOne Streptavidin C1	Invitrogen	Cat# 65001
QIAquick PCR purification kit	Qiagen	Cat# 28104
DNeasy Blood & Tissue Kit	Qiagen	Cat# 69504
Experimental Models: Organisms/Strains		
Bacillus subtilis 168	BGSC	1A1
Bacillus subtilis 168 deletion mutants	This study	BKE or BKK with locus tag numbers
Escherichia coli DH5α	Lab stock	N/A
Escherichia coli Rosetta2 (DE3)	EMD Millipore	Cat# 71400
Escherichia coli BW25113	Baba et al., 2006	N/A
Escherichia coli BW25113 *ΔserB*	Baba et al., 2006	N/A
Recombinant DNA		
pDR240a	This study	N/A
pDR242a	This study	N/A
pDR244	This study	N/A
pDR110a	Rudner lab	N/A
pET28a	EMD Millipore	Cat# 69864
Sequence-Based Reagents		
Primers used in this study are listed in Table S1.	This study	N/A
Software and Algorithms		
Primer3	Untergasser et al., 2012	http://biotools.umassmed.edu/bioapps/primer3_www.cgi
Bowtie2	Langmead and Salzberg, 2012	http://bowtie-bio.sourceforge.net/bowtie2/index.shtml
Iris	Kritikos et al., 2017	https://github.com/critichu/Iris/
Protein BLAST	Altschul et al., 1990	https://blast.ncbi.nlm.nih.gov/Blast.cgi
GSEA	Broad Institute	http://software.broadinstitute.org/gsea
iTOL	Letunic and Bork, 2016	http://itol.embl.de/

CONTACT FOR REAGENT AND RESOURCE SHARING

B. subtilis single gene deletion mutants are available from Bacillus Genetic Stock Center (BGSC, www.bgsc.org) and whole library is available from Addgene (www.addgene.org/Carol_Gross). Further information and requests for other reagents may be directed to, and will be fulfilled by the lead contact, Carol Gross (cgrossucsf@gmail.com).

EXPERIMENTAL MODEL AND SUBJECT DETAILS

B. subtilis 168 strain (BGSC; accession number: 1A1) was used as the wild-type strain for construction of mutant libraries and genetic analysis. Strain numbers of each mutant were assigned as BKK (Kan^R) or BKE (Erm^R) with the locus tag of the deleted gene. Cells were routinely grown in LB medium (1% tryptone, 0.5% yeast extract and 0.5% NaCl) at 37°C with aeration or on LB agar plates. LB medium was supplemented with 7.5 μg/ml kanamycin or 1 μg/ml erythromycin + 12.5 μg/ml lincomycin for selection of Kan^R or Erm^R mutants respectively. *E. coli* K-12 BW25113 and its *serB* deletion mutant (Baba et al., 2006) were used for testing functional compatibility between *E. coli serB* and *B. subtilis ysaA*. Cloning was performed in *E. coli* DH5α.

METHOD DETAILS

Design of Primers

Primers used for construction of gene targeting fragments and cloning of genes were designed by using Primer3 (Untergasser et al., 2012). When *orfA* and *orfB* are separated by >21 bp, the whole ORF is removed, except for its start and stop codons. When *orfA* and *orfB* are separated by <21 bp (e.g. many genes in same operon such as *pdhA* and *pdhB*), the *orfA* deletion leaves 21∼ 23 bp upstream region from the start site of *orf*B. The exact spacing is based on matching the reading frame of the scar after loop-out with stop codon of *orfA*. For translationally coupled genes (e.g. *pyrD* and *pyrF*), the *orfA* deletion maintains a region of 21 -23 bp (depending on reading frame) upstream of the *orfB* start site and the *orfB* deletion maintains the stop codon of *orfA*. When stop codons overlap their intrinsic transcriptional terminators, placing the 3′ end of the antibiotic resistance cassette just prior to the stop codon obliterates the terminator and generate long transcripts that could be antisense RNA for a convergent downstream gene. For example, we were unable to fully delete *yerO* and *ycgJ*, likely because loss of the terminator produced a transcript antisense to the convergent essential *gatA,B,C* and *aroK* genes respectively but could make one ∼30 bp shorter that retained the terminator. All primers are listed in Table S1.

Construction of Single Gene Deletion Mutants

Schematic procedure of construction of single gene deletion mutants is described in Figure 1A. The PCR reactions, transformations and mutant storage steps were performed in microtiter plates using automated liquid handling platforms with in-house protocols designed to minimize cross-contamination.

Generation of Gene Targeting DNA Fragments

Gene targeting DNA fragments were generated by joining PCR of three fragments; antibiotic resistance cassette containing random barcodes, 1kb 5′ and 3′ flaking sequences of targeting gene. For preparation of antibiotic resistance cassettes, PAGE-purified primer pairs Ab-F (5′ GCAGGCGAGAAAGGAGAGVNNVNNVNNVNNVNNVNNVNNGAGGGAGGAAAGGCAGGA 3′, V is A or C or G) and Ab-R (5′ CGAGGCTCCTGTCACTGCNNBNNBNNBNNBNNBNNBNNBCGCCGTATCTGTGCTCTC 3′, B is C or G or T) (0.5 μM final each) were mixed with 10 ng of purified template plasmid (pDR240a for Kan^R and pDR242a for Erm^R) and amplified by PCR under standard condition using Phusion hot-start DNA polymerase (NEB). Amplified Kan^R or Erm^R fragments were purified by gel extraction. For preparation of flanking sequences of target genes, targeting gene specific primer pairs, 5pL-5pR and 3pL-3pR (0.5 μM final each) were arrayed in 384-well PCR plates and mixed with 20 ng of purified *B. subtilis* 168 genomic DNA, and amplified by PCR under standard conditions. Amplified flanking DNA fragments in 384-well plates were purified using the Agencourt AMPure XP (Beckman Coulter) magnetic beads. Antibiotic resistance cassette and 5′ and 3′ flanking DNA fragments (approximately 15 ng of each DNA) were mixed and subjected to the joining PCR in the presence of 5pL and 3pR (0.5 μM final each) under following conditions: 1 min at 98°C; (10 s at 98°C, 20 s at 55°C, 80 s at 72°C) for 30 cycles; 5 min at 72°C using detergent-free HF buffer and Phusion hot-start DNA polymerase. The joined PCR products were directly used for transformation. All high-throughput liquid handling steps were performed using a Biomek FX liquid handling robot.

Transformation, Purification and Storage of Mutants

All *B. subtilis* mutants were constructed using natural competence. Competent cells were prepared by following protocol; Wild-type *B. subtilis* 168 cells were inoculated into 3 ml of MC medium (10.7 g/L K_2HPO_4, 5.2 g/L KH_2PO_4, 20 g/L glucose, 0.88 g/L trisodium citrate dihydrate, 0.022 g/L ferric ammonium citrate, 1 g/L casamino acids, 2.2 g/L potassium glutamate monohydrate, 20 mM $MgSO_4$, 300 nM $MnCl_2$, 20 mg/L L-tryptophan) and incubated at 37°C overnight with aeration. The overnight culture was diluted to an OD_{600} of 0.1 in 30 ml competence medium (10.7 g/L K_2HPO_4, 5.2 g/L KH_2PO_4, 20 g/L glucose, 0.88 g/L trisodium citrate dihydrate, 0.022 g/L ferric ammonium citrate, 2.5 g/L potassium aspartate, 10 mM $MgSO_4$, 150 nM $MnCl_2$, 40 mg/l L-tryptophan, 0.05% yeast extract), then grown in a 125 ml flask at 37°C with shaking (250 rpm) until cells reached OD_{600}∼1.5. 120 μl of culture was then mixed with 10 μl of gene targeting PCR fragments arrayed in a deep 96-well plate, covered with a breathable film, and incubated at 37°C with shaking (900 rpm). After 2 hr incubation, cells were plated on LB agar containing selective antibiotics (7.5 μg/ml kanamycin or 1 μg/mL erythromycin, and 12.5 μg/ml lincomycin [by activity]). After 16∼24 hr incubation, four single colonies from each plate were purified by restreaking on new selection plate; two of them were stored in 15% glycerol at -80°C.

Removal of Antibiotic Resistance Cassette from BKK and BKE Strain

BKK or BKE strain was transformed with pDR244 (temperature-sensitive plasmid with constitutively expressed Cre recombinase). Transformants were selected on LB agar plate supplemented with 100 μg/mL spectinomycin at 30°C. Transformants were then streaked on LB agar plates and incubated at 42°C. Cells from the edge of single colonies were then restreaked on LB, LB supplemented with kanamycin (for BKK) or erythromycin and lincomycin (for BKE), and LB supplemented with spectinomycin. A strain that grew on LB agar plate, but not on LB agar plates supplemented with antibiotics, had lost pDR244 and antibiotic resistance cassette. Markerless deletion was confirmed by PCR with primers flanking the deletion (5pL and 3pR).

Validation of New Essential and Non-Essential Genes

As described in RESULTS AND DISCUSSION, essential genes were defined based on inability to obtain viable transformants using two independent, validated PCR products. New essential gene candidates were confirmed using a standard complementation protocol. The ribosome binding site and ORF of a candidate gene was cloned into pDR110a integration plasmid where its expression is under control of IPTG inducible promoter. After transformation of the plasmid containing the cloned gene into wild-type for ectopic

Please cite this article in press as: Koo et al., Construction and Analysis of Two Genome-Scale Deletion Libraries for *Bacillus subtilis*, Cell Systems (2017), http://dx.doi.org/10.1016/j.cels.2016.12.013

expression of new essential gene candidate from *amyE* locus, the ORF of native gene was replaced with Kan^R or Erm^R cassettes by transformation of gene targeting DNA fragment in medium supplemented with IPTG. Primers used in construction of complementation strains are listed in Table S1. If the gene was previously annotated as essential, we confirmed that the new non-essential gene mutants lacked a copy of the gene that was deleted. Two sets of PCR were carried out using different combination of primers, reaction A with 3pR and antibiotic resistance cassette- specific primers (5′ AGTAAGTGGCTTTATTGATCTTGGG 3′ for Kan^R and 5′ CCTTAAAACATGCAGGAATTGACG 3′ for Erm^R) and reaction B with deleted gene-specific primer pair. Gene deletions were confirmed by ~1.2 kb PCR product from reaction A and no product from reaction B.

Identification of Mutant-Specific Barcodes

Pooling Mutants and Preparation of Genomic DNA

Each mutant was inoculated into deep 96-well plates containing 200 μl LB supplemented with 3.5 μg/ml kanamycin (for Kan^R) or 0.5 μg.ml erythromycin (for Erm^R) from frozen stocks using a BioMek FX liquid handling robot and incubated in an Infors incubator at 30°C overnight with shaking at 900 rpm. 5 μlof each mutant culture was pooled in deep 96-well plates as described in Figure 1A. Mutants in the same pool were combined in one tube and genomic DNA was purified using the Qiagen DNeasy Blood & Tissue kit.

Preparation of Sequencing Library

Deep sequencing samples were prepared as previously described with some modifications for identification of the gene associated barcode (Son and Taylor, 2011). Genomic DNA from each pool was sheared using a Bioruptor (UCD-200) sonicator to yield fragments with a mean length of 250 bp. The sheared DNA was concentrated using a Qiagen PCR purification kit, and end-repair, dA tailing and adapter ligation were carried out as previously described. For enrichment of barcodes and their flanking region, total 72 reactions (9 pools × 2 libraries × 2 barcodes × 2 clones) of first-round PCR were performed using primers, biotinylated P1_UPs (Kan^R or Erm^R library-specific indices are included) and P2_INDs (including pool specific indices are included). Amplified biotinylated products were purified using Dynabeads MyOne Streptavidin C1 (Invitrogen). First-round PCR products were further amplified using the Illumina paired-end primer PE2.0S and PE1.0 and DNA fragments of 200-600 bp were size selected and purified by agarose gel electrophoresis prior Illumina sequencing. Sequences of primers used for preparation of sequencing libraries are listed in Table S1.

Analysis of Barcodes

Mutant specific barcodes were identified by mapping the sequencing reads onto the genome sequence of *B. subtilis* using Bowtie2 (Langmead and Salzberg, 2012). Cross-contamination was assessed by the presence of mutant barcodes in pools that should not contain the mutant.

Quality Control of Library

We established four quality control standards and replaced strains failing any standard.

(1) Pools expected to lack a particular mutant must have minimal barcode reads originating from that mutant (the smaller of ≤10 reads or ≤ 5% barcode reads in the correct group). We found only 2 cases of this problem-suggesting little cross contamination, a proposition validated by our phenotyping analysis.
(2) Barcodes uniquely identified the antibiotic replacement cassette with which it was associated.
(3) The barcode length was > 17bp, the UP1 and UP4 universal priming sequences were intact, and the appropriate size of the scar following excision of antibiotic resistance cassette was maintained.
(4) The strains were wild-type at the SpoIIE locus.

High-Throughput Growth Phenotype Screen

The screen was carried out as described previously for *E. coli* chemical genomics (Nichols et al., 2011) with modifications optimized for *B. subtilis*. Plates for screening were allowed to dry for two days. Erm^R and Kan^R libraries were independently re-arrayed in 384-well plates using a Biomek FX liquid handling robot (Beckman Coulter) and stored as glycerol stock. To screen each library, cells were pinned from glycerol stocks onto rectangular LB agar plates in 384-format using a Singer Rotor robot, then four 384-format plates were combined and pinned to 1536-format. For each screen, exponentially growing cells in 1536-format were then pinned to LB or defined media plates and incubated for 6~48 hr depending on their growth conditions. Composition of defined media was described in Table S4. All plates were incubated in a humidified incubator. Plates were imaged using a Powershot G10 camera (Canon) when at a time point at which fitness differences were apparent but growth had not saturated. The calculation of RF and nRF was carried out as described in Quantification and Statistical Analysis.

High-Throughput Sporulation Assay

Exponentially growing cells in 1536-format on LB agar plates were pinned to sporulation medium agar plates (0.2% succinate, 0.1% glutamate, 1X $S7_{50}$ salts, 40 μg/ml L-tryptophan, 1X metals, 10 μM $MnCl_2$, 0.1X AAA, 0.1X FAA, 0.1X BAA, 0.25X ACGU, 0.1X vitamin mix, 2% agar). Sporulation was measured after incubation of plates at 37°C in a humidified incubator for 45 hr. Plates were imaged using a Powershot G10 camera (Canon) and sporulation scores were quantified using Iris (Kritikos et al., 2017), which measures the dark brown pigmentation at a defined area around the colony center.

High-Throughput Double Gene Mutant Generation

Erm^R library was pinned from glycerol stocks onto rectangular LB agar plates in 384-format using a Singer Rotor robot, then pinned again onto MC agar plates and incubated overnight. Each of the Erm^R mutants arrayed on MC agar plates were resuspended in liquid competence medium using a Singer Rotor robot. 20 μl transformation reactions in shallow 384-well plates were set as following: 4 μl of cells resuspended in competence medium, 4 μl of donor genomic DNA resuspended in competence medium (*hisC::kan*^{R}, final 1 μg/ml), and 12 μl of competence medium. Each plate was covered with a breathable film and incubated for 16 hr without shaking. For enrichment of transformants, 5 μl of LB with kanamycin (final concentration, 3.5 μg/ml in 25 μl) was added to each well and incubated for 6 hr further. Following enrichment for transformants on kanamycin, transformants were first selected on LB supplemented with kanamycin followed by LB supplemented with kanamycin and erythromycin. Double mutants (Kan^R and Erm^R) were screened to identify the aminotransferase gene performing the final step of Phe and Tyr biosynthesis by pining on selective minimal media. All plates in each step were incubated at 37°C in a humidified incubator. For confirmation of competence genes identified in 1st genome-wide screen, 88 candidate mutants and 70 mutants missing from 1st screen due to no or poor growth in MC medium were rearrayed in two 96-well plates. The following modifications were applied to second screen; 1) MC medium was supplemented with nucleotide bases and vitamins, 2) Reactions were carried out in shallow v-bottom 96-well plates, and 3) two different donor genomic DNA (*hisC:kan* or *amyE:kan*) with higher concentration (final 3 μg/ml) were tested.

Identification of the Function of YsaA

Metabolic Suppression Profiling

The profiling was carried out as previously described (Zlitni et al., 2013), with modification of the metabolic suppression array. Cells exponentially growing in LB medium were collected and washed with glucose minimal medium by mild centrifugation. Cells resuspended in glucose minimal medium were diluted to an OD_{600} of 0.01 in 150 μl of each culture medium in 96 well plate described in Figure 4A. Plate was covered with a breathable film and incubated at 37°C with shaking (900 rpm). OD_{600} of each culture was measured after 18 hr.

Cloning, Overexpression and Purification of YsaA

ysaA was amplified from *B. subtilis* 168 genomic DNA using primers ysaA-F3 (CAACGgctagc AAAGCCGTATTTTTTGATTTAGAT) and ysaA-R3 (AACTCggatccCATTTCACTTGATGAGTTTGTG) to create flanking *Nhe*I and *BamH*I sites. Purified PCR product digested with *Nhe*I and *BamH*I was inserted into the pET28a vector.

YsaA was overexpressed in *E. coli* Rosetta2 (DE3). Overnight cultures were diluted 1:100 into fresh LB medium containing 20 μg/ml kanamycin and 30 μg/ml chloramphenicol, and grown aerobically at 30°C. When the cultures reached OD_{600} of 0.4, expression of YsaA was induced by addition of IPTG to a final concentration of 1 mM and growth continued at 30°C with aeration for 2 hr. Purification of YsaA was carried out as described previously (Huang et al., 2015). Cells were suspended in lysis buffer [20 mM HEPES (pH 7.5), 500 mM NaCl, 20 mM imidazole, and 10% (vol/vol) glycerol] and lysed by sonication. The lysate was clarified by centrifugation at 35,000 × *g* for 30 min. Clarified lysate was loaded onto an ÄKTAxpress FPLC (GE Healthcare). Lysate was loaded onto a 1 mL HisTrap FF column (GE Healthcare), washed with 10 column volumes of lysis buffer, and eluted in buffer containing 20 mM HEPES (pH 7.5), 500 mM NaCl, 500 mM imidazole, and 10% glycerol. The purified sample was loaded onto a HiLoad S200 16/60 PR gel filtration column that was equilibrated with SECB buffer [20 mM HEPES (pH 7.5), 150 mM NaCl, 10% (vol/vol) glycerol, and 5 mM DTT]. Peak fractions were collected and protein was analyzed by SDS/PAGE, snap-frozen in liquid nitrogen, and stored at -80°C.

Enzyme Kinetics

For steady-state kinetic characterization, purified YsaA was diluted to 5 nM into an assay buffer (25 mM HEPES, pH 7.5, 0.3 mM TCEP, 5 mM $MgCl_2$). The steady-state kinetic parameters (K_m and k_{cat}) for each substrate were determined from initial reaction velocities measured at varying substrate concentrations (0.5 – 5 K_m). The assay was carried out in assay buffer with Biomol Green reagent for phosphate detection in a total volume of 50 μl in a 96-well microtiter plate. Enzyme and substrate were incubated at 25°C for various time points and reactions were quenched by the addition of 100 μl Biomol Green reagent to each well. The assay plate was incubated at room temperature for 60 minutes to allow color to fully develop. The OD_{620} was measured on a Molecular Devices SpectraMax M5 microtiter plate reader. Inorganic phosphate release was quantified by comparison to a standard curve constructed by using a range of KH_2PO_4 concentrations diluted in deionized distilled water. Data were fit to the following equation using Prism:

$$v_o = V_{max}[S]/K_m + [S] \qquad \text{(Equation 1)}$$

Here, v_o is the initial velocity, V_{max} the maximum velocity, [S] the substrate concentration and K_m the Michaelis-Menten constant. The value for k_{cat} was calculated from the equation $k_{cat} = V_{max}$ [E], where [E] is the protein concentration in the assay. The steady-state kinetic constants are reported in Figure 4G.

QUANTIFICATION AND STATISTICAL ANALYSIS

Calculation of Relative Fitness, RF and nRF

Mutants arrayed in high density on agar plates (1536 mutants/plate) were grown for 6~48 hours depending on conditions. Fitness was measured by the colony opacity of each mutant determined with *B ssubtilis* optimized Iris colony sizing software, and spatial effects on plates were corrected (Kritikos et al., 2017). The RF of each mutant was calculated as: RF = (colony opacity of

Please cite this article in press as: Koo et al., Construction and Analysis of Two Genome-Scale Deletion Libraries for *Bacillus subtilis*, Cell Systems (2017), http://dx.doi.org/10.1016/j.cels.2016.12.013

mutant)/(median colony opacity of the plate). The average RF calculated from three technical replicates is presented in Table S4. The nRF of each mutant represents the RF in condition X relative to its RF in the Standard Condition (LB 37°C).

Identification of Auxotrophs

Auxotrophs were experimentally identified by determining library fitness in glucose-ammonium minimal medium, supplemented with tryptophan to complement the *trpC* mutation in *B. subtilis* 168. A total of 93 strains were defined as auxotrophic according to their nRFs of both libraries. Eighty strains were unable to grow (average nRF of Erm^R and Kan^R is less than 0.1 and one of their nRF is 0). Thirteen additional strains showed some growth (average nRF of Erm^R and Kan^R is between 0.1 and 0.3, but none of their nRF is higher than 0.3), likely due to nutrient carryover.

Calculation of Relative Sporulation Score, rSS

Sporulation was measured after growing the arrayed libraries for 45 hours on sporulation medium agar plates. Sporulation scores were assigned based on the color intensity at center of each colony (Figure 4A), as determined with Iris. Normalized sporulation scores were calculated by normalizing replicate plate bias. Positional effects were addressed by separately normalizing values of colonies positioned in the 4 outermost rows and columns of the colony array. rSS was calculated by following equation, rSS = (sporulation score of mutant)/(median sporulation score in plate). Dependence of the sporulation score on colony size (mutant fitness) was assessed, and a minimum size threshold was set at 1100 pixel (Table S5). Mutant values were averaged separately for the Erm^R and Kan^R libraries and compared. Mutants with discordant clones and mutants that were not viable in either library were discarded. Erm^R and Kan^R library scores for remaining mutants were averaged into per-mutant scores.

Analysis of Dataset

Pre-ranked GSEA using default values (Subramanian et al., 2005) was performed on the mean centered RF, nRF, or rSS values to test for enrichment of *B. subtilis* COG, prophage genes and sporulation sigma regulon genes using the Broad Institute GSEA desktop application. To test for enrichment in gene lists and strand bias of auxotrophic gene, the Bonferroni corrected hypergeometric test was used. To test for conservation of genes grouped by their sporulation phenotypes among other spore-forming bacteria, the Chi-squared test with Yates' continuity correction was used.

Databases for *B. subtilis* gene annotation, COG and regulation were downloaded from Microscope, EggNog and SubtiWiki (Huerta-Cepas et al., 2016; Michna et al., 2014; Vallenet et al., 2013). COG assignments for some genes were updated and modified as needed.

Conservation Analysis

Conservation of genes across species was performed using Protein BLAST (Altschul et al., 1990). All protein sequences for the selected species were downloaded from the RefSeq database Release 78 (O'Leary et al., 2016) using the rentrez R package. Subsequently, a BLAST database was made for each species, and Protein BLAST was used to extract protein similarities for each query gene. We defined gene conservation by two-step procedure. First, conserved genes were identified by setting a bit score threshold at 50, and a sequence identity threshold of 30%. Second, we validated them based on their functional annotations.

Species phylogenetic trees were created by hierarchical clustering pairwise species distances. Distances used were acquired using a set of universal marker proteins (Mende et al., 2013).

DATA AND SOFTWARE AVAILABILITY

Software

The Iris image analysis software was used to automatically quantify colony size and sporulation. Binary distribution and source code are freely available at https://github.com/critichu/Iris/.

Cell Systems, Volume *4*

Supplemental Information

Construction and Analysis of Two Genome-Scale Deletion Libraries for *Bacillus subtilis*

Byoung-Mo Koo, George Kritikos, Jeremiah D. Farelli, Horia Todor, Kenneth Tong, Harvey Kimsey, Ilan Wapinski, Marco Galardini, Angelo Cabal, Jason M. Peters, Anna-Barbara Hachmann, David Z. Rudner, Karen N. Allen, Athanasios Typas, and Carol A. Gross

SUPPLEMENTAL FIGURES

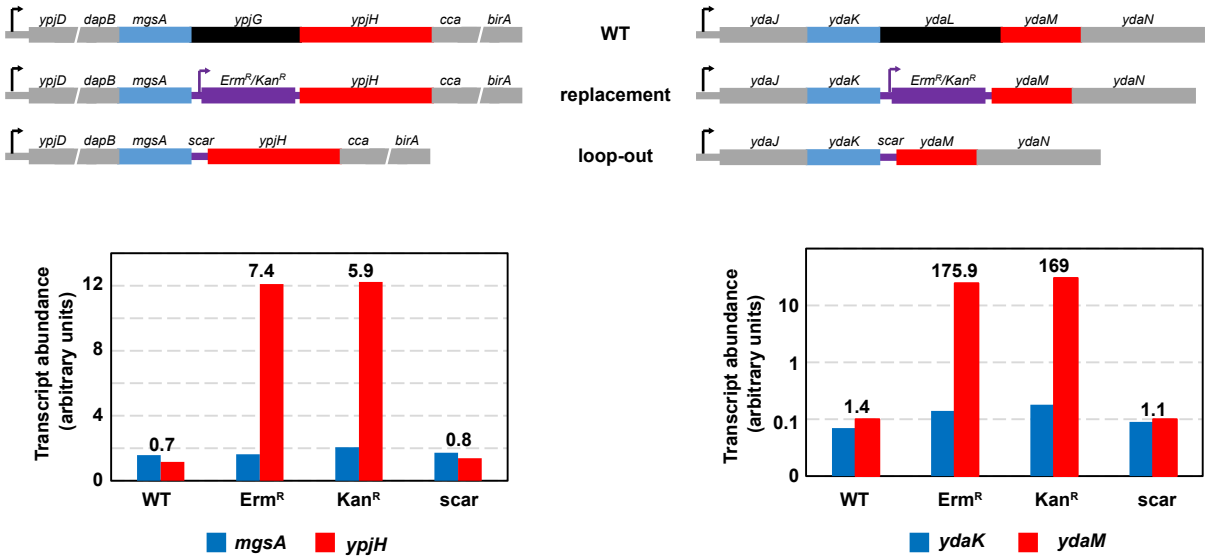

Figure S1. The antibiotic replacement constructs induce overexpression of downstream genes in the same transcriptional unit, related to Figure 1

The *ypjG* (left) and *ydaL* (right) genes, residing respectively in the *ypjD* and *ydaJ* operons, were investigated. The transcript abundance of genes directly upstream and downstream of *ypjG* and *ydaL* were assessed by qRT-PCR for the wild-type strain, the Erm^R and Kan^R replacements, and the marker excised (scar) mutant. The ratio of transcript abundance of the downstream/upstream transcript indicates extent of overexpression mediated by transcription originating from the antibiotic resistance cassette, and is indicated above the bar graphs for each strain. When endogenous transcription of an operon is low, expression initiated from the promoter driving the antibiotic resistance cassette in an upstream gene will cause overexpression of downstream genes, which could result in altered phenotypes. For example, antibiotic replacements of the genes (*dacF*, *spoIIAB* and *xtrA*) upstream of *spoF* and *xpf* σs resulted in translucent colonies, that rapidly accumulated suppressors inactivating the σs, likely removing toxicity resulting from their overexpression. Discrepant phenotypes of Erm^R and Kan^R replacements may reflect differential effects on downstream gene expression. For example, only the Kan^R replacement of *kinA* had a significant growth defect. The antisense Kan^R transcript may inhibit the convergently transcribed essential *patA* gene more efficiently than the Erm^R one. These overexpression phenotypes can be eliminated by Cre-mediated excision of antibiotic resistance cassette.

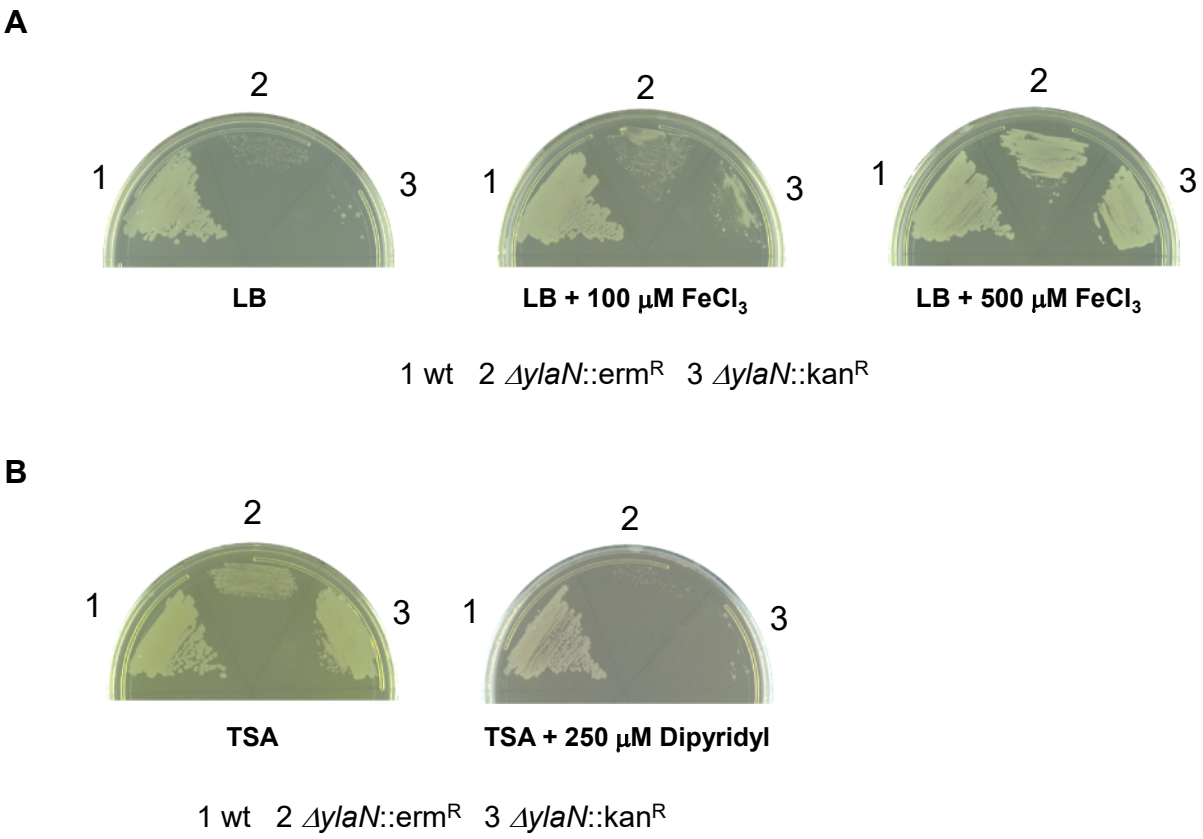

Figure S2. *ylaN* requires high concentration of iron for growth, related to Figure 2

The *ylaN* mutant requires additional iron to grow in LB. That *ylaN* is considered non-essential in *Staphylococcus aureus* (Santiago et al., 2015) is likely related to the high concentration of iron in standard *S. aureus* TSA growth medium, which is sufficient to support the growth of the *B. subtilis ylaN* mutant. Both Erm^R and Kan^R *ylaN* were tested for growth in various media.

(A) The growth of *ylaN* is dependent on the iron concentration.

(B) TSA supports the growth of *ylaN* (left) except when iron was depleted using the, 2,2′-dipyridyl chelator at a concentration that permitted growth of wild-type cells (right). Thus, the ability of *ylaN* to grow on TSA is a consequence of the high iron concentration in the medium.

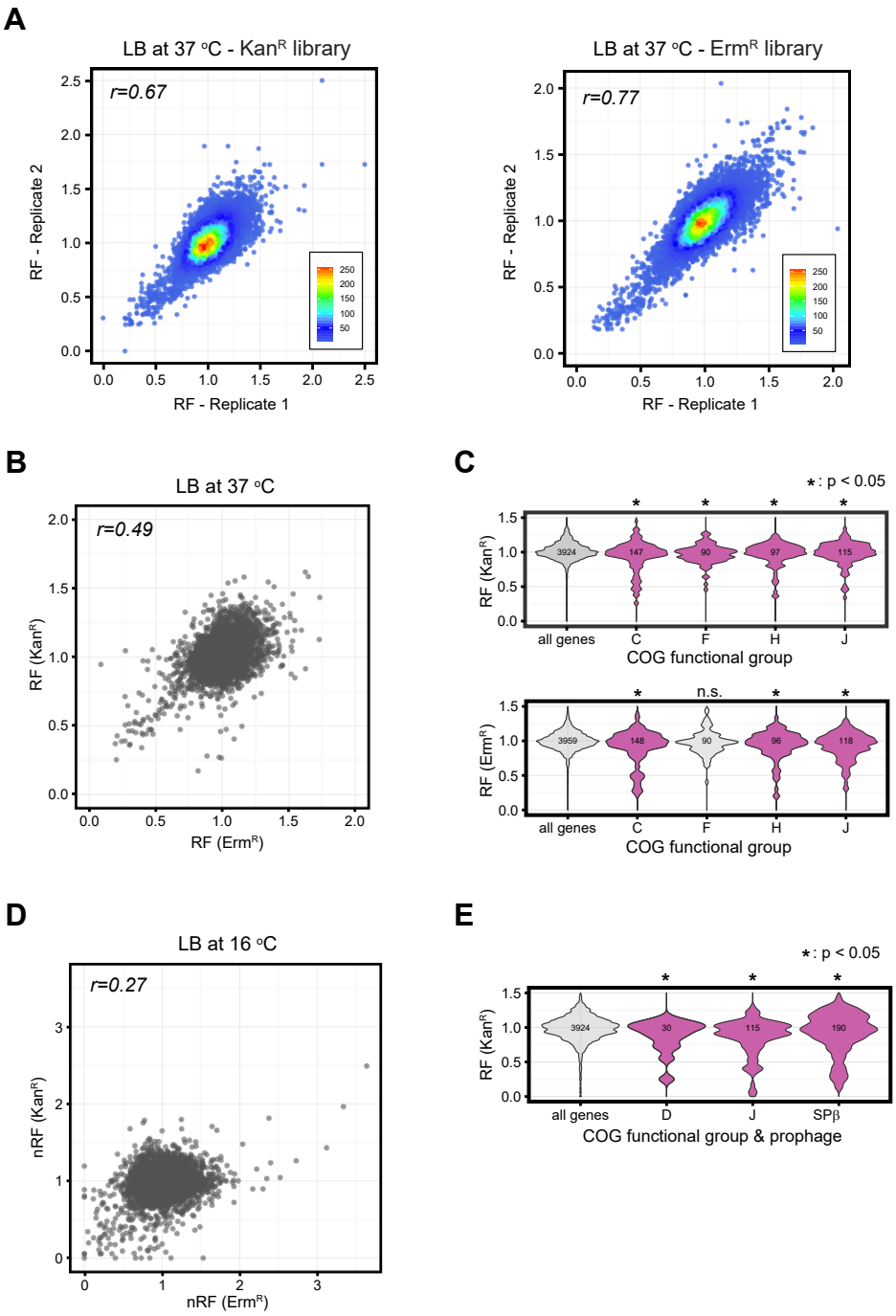

Figure S3. Strain fitness in standard growth condition and low temperature, related to Figure 3

(A) Heat map representation of scatter plot comparing RF in LB at 37˚C of replicates 1 and 2 of Kan^R (left) and Erm^R (right) library across entire data set. Zero RF value from both replicates represents the mutants that we failed to recover from frozen stock due to technical issue or their severe growth defect without supplement (e.g. heme biosynthesis mutants). These mutants were also not screened in other conditions and removed from further analysis.

(B) Scatter plot of the RF of Erm^R and Kan^R mutants in LB at 37˚C. Note that screening of Erm^R library was performed earlier than that of Kan^R library with different batches of media, which might result in less agreement of the fitness phenotype between two libraries.

(C) Functional groups enriched in slower growing mutants in LB at 37˚C. *, p-value <0.05); n.s., not significant. C, energy production and conversion; F, nucleotide transport and metabolism; H, coenzyme transport and metabolism; J, translation, ribosome structure and biogenesis. Distribution of RFs of genes in enriched functional categories in Kan^R (top) and Erm^R (bottom) libraries is shown by a violin plot.

(D) Scatter plots of the nRF of Erm^R and Kan^R mutants in LB at 16˚C.

(E) Functional groups enriched in slower growing mutants LB at 16˚C ($p<0.05$). Our analysis is based solely on the Kan^R library, as Erm^R library phenotypes were noisy (Figure S3D) in this condition and methylation of ribosomal RNA in Erm^R strains might affect the results. GSEA indicated enrichment of translation/ribosome structure and biogenesis (J), cell cycle control/division/chromosome partitioning (D) and SPβ prophage genes. As the SPβ cured PY79 strain grows equivalently to 168 strain at low temperature, the *cs* phenotype of SPβ prophage gene deletions likely results from toxicity caused by overexpression of downstream genes. Distribution of RFs of genes in each functional category in the Kan^R library is shown by violin plot.

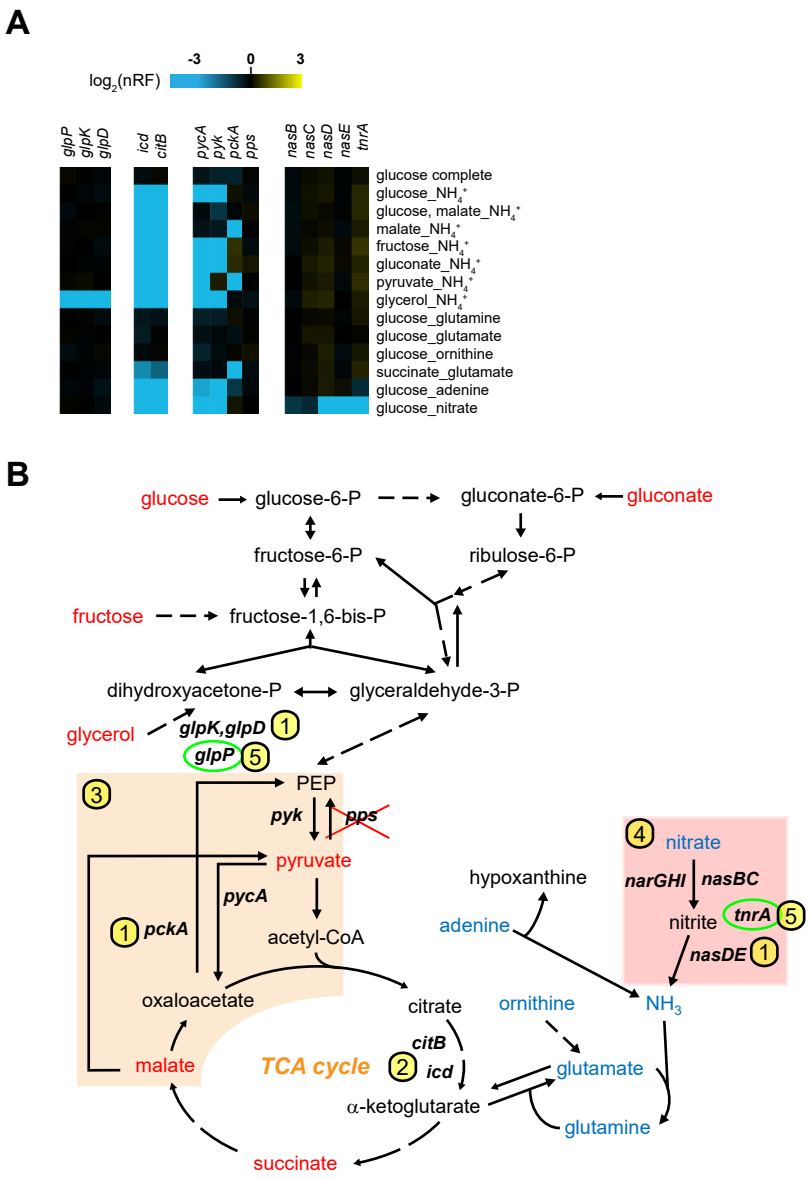

Figure S4. The C (red) and N (blue) sources used in this screen and their metabolism in *B. subtilis*, related to Figure 3

(A) Zoomed-in heat maps of nRFs of the mutants discussed in (B).

(B) Pathways catalyzed by metabolic genes required for utilization of particular C and N sources. Solid arrows indicate direct conversion between two metabolites; dashed arrows indicate that there are intermediate metabolites.

1, Genes encoding enzymes essential for utilization of specific C or N sources. *pckA* for malate, pyruvate and succinate, *glpD* and *glpK* for glycerol, *nasD* and *nasE* for nitrate. More cases are listed in Table S4.

2, Auxotrophy bypass. A few glucose-minimal auxotrophs grow on other C or N sources that bypass the need for that function (e.g. glutamate bypasses the need for *citB* and *icd* mutants).

3, The PEP-pyruvate-oxaloacetate node is highlighted in orange. By comparing phenotypes in malate and pyruvate-minimal media, we showed that in *B. subtilis*, phophoenolpyruvate (PEP), an essential metabolic intermediate, is synthesized only from the oxaloacetate pathway (using *pckA*) whereas in *E. coli*, PEP is also synthesized from pyruvate (using *pps*). The critical observation is that in *B. subtilis*, *pckA* is essentially required for growth in both malate and pyruvate minimal media whereas *pps* mutant has no phenotype (see heat maps of nRFs in A). The red X on *pps* denotes our finding that *pps* is not functional in this reaction.

4, Nitrate assimilation pathway. The ability of *nasB* and *nasC* mutants to grow on nitrate, albeit at reduced efficiency (nRF, ~0.5), indicates that a 2nd nitrate reductase, most likely NarGHI must also carry out this step. Conversely, the inability of *nasD* and *nasE* mutants to grow on nitrate indicates that NasDE is the sole nitrite reductase complex.

5, Transcriptional regulators required for utilization of specific C or N sources, GlpP for glycerol and TnrA for nitrate and probably also nitrite indicated by green circles. GlpP is transcriptional antiterminator of the *glpT-glpQ* and *glpF-glpK-glpD* operons. TnrA is the global regulator of nitrogen metabolism that activates transcription of *nasB-nasC-nasD-nasE* under nitrogen limitation (Yoshida et al., 2003).

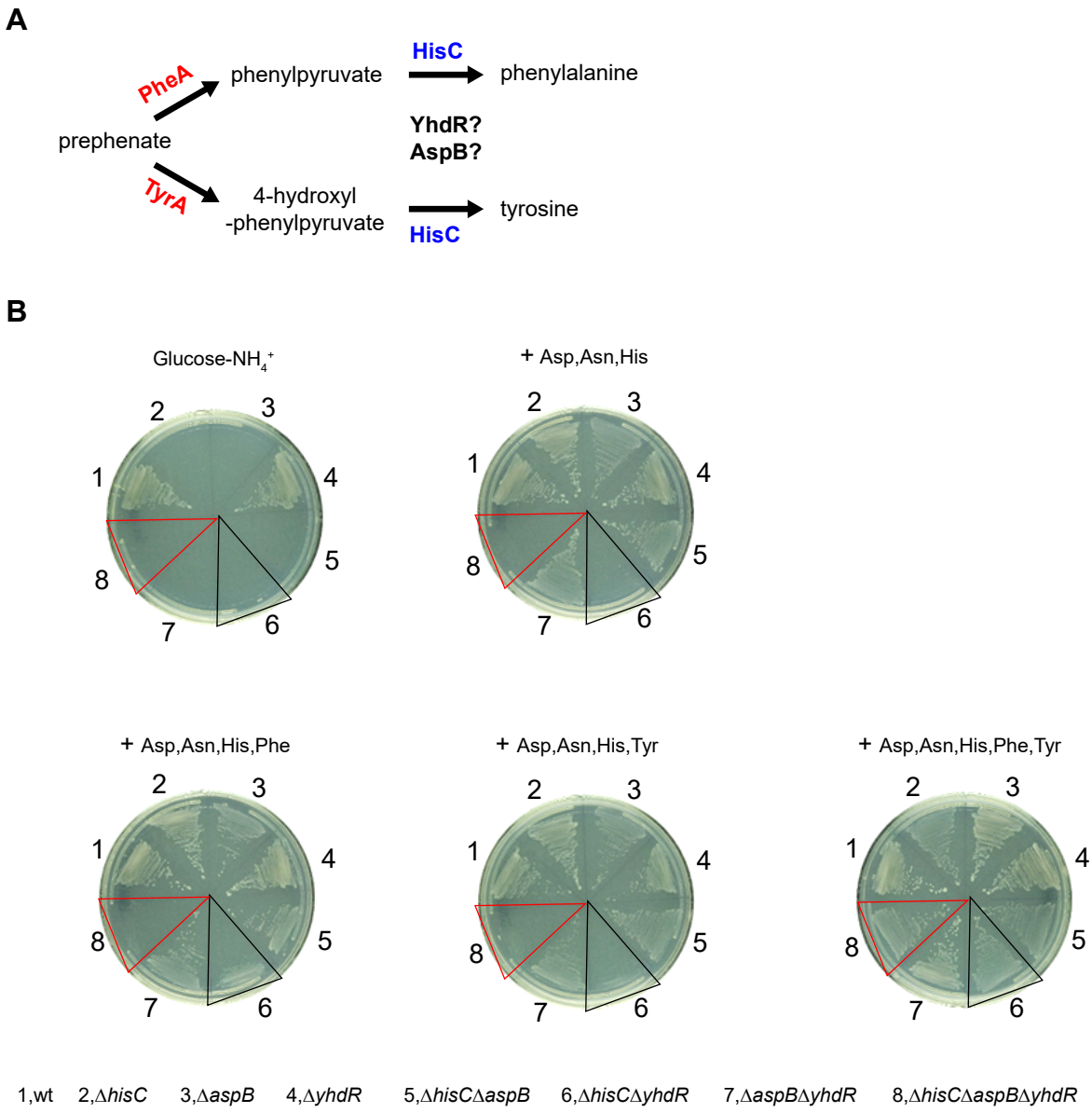

Figure S5. Identification of genes performing the final step of Phe and Tyr biosynthesis, related to Figure 5

(A) Biosynthesis pathways of Phe and Tyr. In addition to its role in histidine biosynthesis, HisC carries out the last step of phenylalanine and tyrosine biosynthesis. As *hisC* strains are not defective in either phenylalanine or tyrosine biosynthesis, additional enzymes must also carry out these functions (Nester and Montoya, 1976).

(B) We identified the gene(s) contributing these redundant functions from our genome-scale *hisC::kan* double mutant screen (Table S6). A double mutant deleted for both *hisC* and the redundant function should require supplementation with His+Phe+Tyr rather than His only. Of the four mutants meeting this criterion, three were eliminated because they catalyzed upstream reactions required for Phe and Tyr production (*pheA*, *aroC and tkt*). The remaining gene, *yhdR*, is annotated as a putative aspartate aminotransferase gene (UniProt, 2015), making it feasible that *yhdR* encodes the redundant Phe and Tyr aminotransferase. The *hisC-yhdR* double mutant (indicated by black triangle) grew moderately with Phe/His but poorly with Tyr/His supplementation, suggesting that YhdR is important for both reactions but contributes more to Phe than Tyr synthesis, thereby implicating yet an additional enzyme. Based on sequence conservation, the KEGG database recently suggested that AspB, along with YhdR, catalyzed this step (Kanehisa et al., 2014). We therefore tested *aspB* and found that although the *hisC/aspB* double mutant did not have a growth defect in media lacking either Phe or Tyr, the *hisC/aspB/yhdR* triple mutant (indicated by red triangle) grew only with both Phe and Tyr supplementation. We conclude that the product of *yhdR*, renamed *pheC*, is one of the two major aminotransferase catalyzing this reaction. AspB plays a minor catalytic role and is necessary only in the absence of both *hisC* and *pheC*. Each single, double and triple mutant (indicated by number) was grown in glucose minimal media supplemented with the designated amino acids. All media had Asp and Asn for optimal growth of *aspB*.

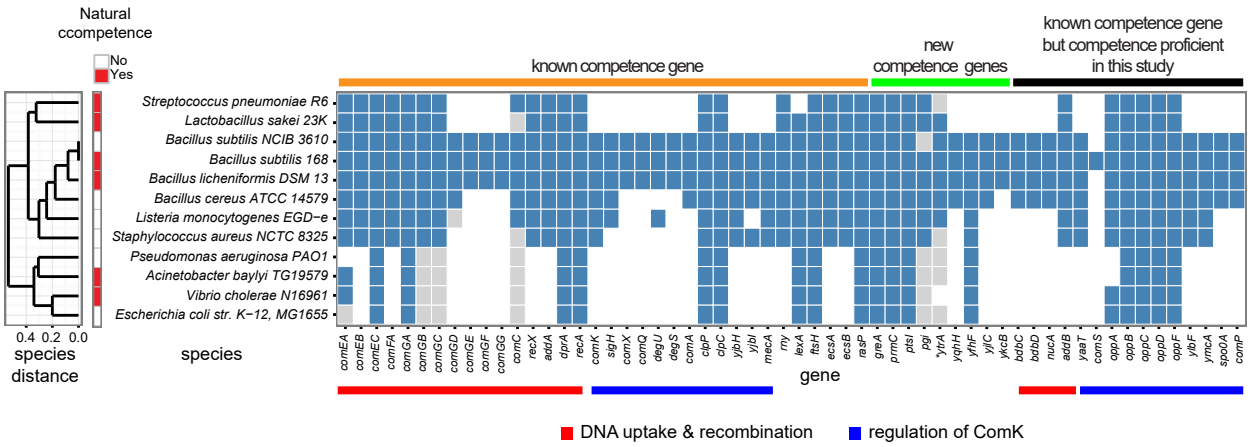

Figure S6. Conservation of competence genes in other naturally transformable and non-transformable bacteria, related to Figure 5

Conservation analysis was performed as described in STAR Methods. Species are shown on the phylogenetic tree (left), and genes are grouped according to their competence phenotype (top) and role in transformation (bottom). Naturally transformable species are indicated by red square between phylogenetic tree and species name. The presence of an ortholog for a given gene in a given species is indicated by a blue square. The presence of a functional analog for a given gene is indicated by a gray square.

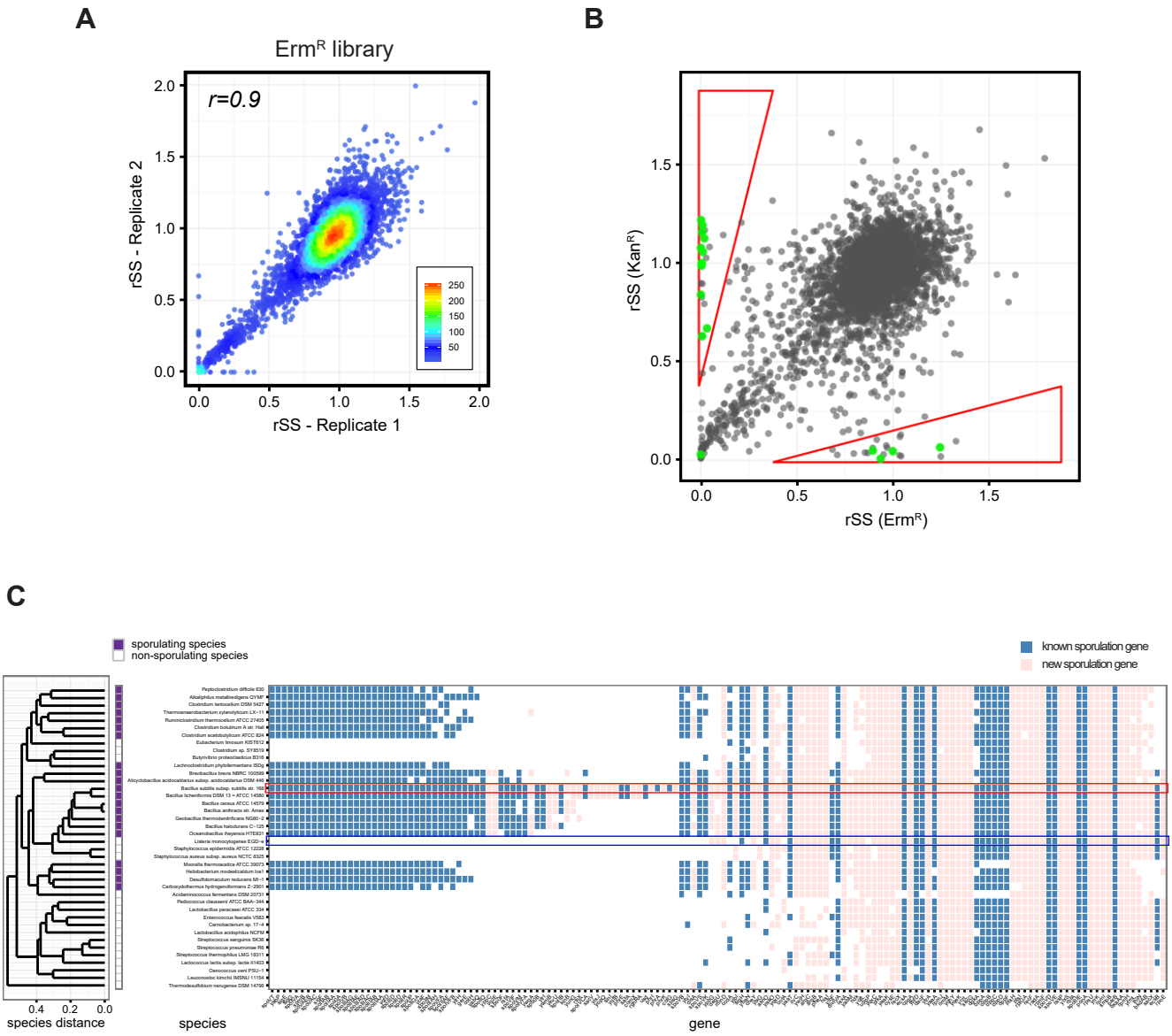

Figure S7. Reproducibility of genome-wide sporulation assay, related to Figure 6

(A) Heat map representation of scatter plot comparing sporulation scores of replicates 1 and 2 of Erm^R library across entire data set.

(B) Scatter plot comparing normalized sporulation scores of Erm^R and Kan^R mutants across the entire data set. Mutants in red triangles show highly discrepant sporulation scores between Erm^R and Kan^R, with one sporulating normally and the other not sporulating (Table S6). We retransformed the antibiotic marked deletion of 13 Erm^R and 5 non-sporulating Kan^R mutants into a wild-type strain and in each case restored sporulation. In contrast, the strain maintained its nonsporulating phenotype when transformed with the other gene replacement. These results suggested that the sporulation phenotype discrepancy between two libraries resulted from a secondary mutation present at another locus in one of the two antibiotic replacements. Whole genome sequencing of 7 Erm^R mutants identified a C to T change at 72,473 (coordinate) that results in SpoIIE L646F, a known non-sporulating mutation (Barak et al., 1996). We subsequently established that *spoIIE* locus of the other 11 nonsporulating Erm^R and Kan^R mutants had the mutation. This result strongly suggested that our wild-type stock had a very low level of contamination by a *spoIIE* mutant. These mutants were removed from gene set enrichment analysis. All discrepant non-sporulating mutants were reconstructed by retransformation into the wild-type strain, and confirmed to be sporulation proficient later.

(C) Conservation of sporulating genes in other bacteria. Conservation analysis was performed as described in STAR Methods. Species are shown on the phylogenetic tree (left), and genes are grouped by new and previously known sporulation genes (top). Sporulating species are indicated by purple square between phylogenetic tree and species name. The presence of an ortholog for a given gene in a given species is indicated by a blue square. For comparison, *B. subtilis* and *L. monocytogenes* are highlighted by red and blue rectangle respectively.

SUPPLEMENTAL TABLES

Table S1. Primers and antibiotic resistance cassettes used in this study, related to Figure 1, 2, 3, 4, 5, and 6
List of primers used for construction of single gene deletion strain (A), list of primers used for construction of complementation strains (B), list of primers used for identification of barcodes (C), and sequence of antibiotic resistance cassettes (D).

Table S2, List of mutant specific barcodes, related to Figure 1

Table S3. Essential genes in *B. subtilis* and their conservation in other bacteria, related to Figure 2
List of essential genes defined in this study (A), changes in our essential gene set compared to SubtiWiki (B), and comparison of essential genes in *B. subtilis*, *S. sanguinis*, *S. aureus* and *E. coli* (C).

Table S4. Genome-wide growth phenotypes in several conditions, related to Figure 3
Growth medium (A), list of fitness scores of the mutants at different temperature and in minimal media supplemented with different C and N source (B), cold-sensitive mutants (C), auxotrophic genes in *B. subtilis* (D), comparison of auxotrophic genes in *B. subtilis* and *E. coli* (E), genes required for utilization of particular C and N sources (F), and list of mutants with high chance of suppressive mutation (G).

Table S5. Genome-wide competence and phenylalanine/tyrosine aminotransferase screen, related to Figure 5
Genome-wide screen for aminotransferase gene for Phe and Tyr synthesis as well as competence mutant (A), list of competence defective mutants identified in this study (B), transformability of mutants of known competence mutants in this study (C) and conservation of competence genes in other bacteria (D).

Table S6. Genome-wide sporulation phenotype screen, related to Figure 6
List of sporulation scores of the mutants (A), list of sporulation defective mutants identified from this study (B), list of the disqualified mutants due to small size of colony (C), list of the mutants showing discordant rSS between Erm^R and Kan^R version (D) and conservation of sporulation genes in other bacteria (E).